# Wobbling motion triaxial nuclei

S. Frauendorf

University of Notre Dame, USA

CWAN'23, July 10, 2023

In collaboration with:
Q. B. Chen, East China Normal University, Shanghai, China
J. Sheikh, Nazira Nazir, University of Kashmir, India
S. P Rouoof, S. Jehangir, N, Rather, Islamic University, India
G. H. Bhat, S. P College, Cluster University, India

Layout:

Triaxial Rotor

One, two particles + Triaxial Rotor

Triaxial Projected Shell Model

# Triaxial Rotor Model (TR)

$H_{TR} = \frac{\hat{R}_s^2}{2\Im_s} + \frac{\hat{R}_m^2}{2\Im_m} + \frac{\hat{R}_l^2}{2\Im_l}$, is diagonalized in the discrete basis of axial-rotor states

$|RRK>$ of good angular momentum $R$, projection $R$ on the z-lab axis

and projection $K$ on the $l$- body axis, $-R \le K \le R$.

$\hat{R}^2 |RRK>= R(R+1)|RRK>, \hat{R}_z |RRK>= R|RRK>, \hat{R}_l |RRK>= K|RRK>,$

TR eigenstates: $|RR\nu>= \frac{1}{\sqrt{2}} \sum_K c_K^{(\nu)} |RRK>$, $K$ even, $c_{-K}^{(\nu)} = (-)^R c_K^{(\nu)}$ : $D_2$ symmetry

represented by the discrete probability amplitudes $<RRK|RR\nu>= c_K^{(\nu)}$

$K-$ plots show the probability distributions $P(K) = \left(c_K^{(\nu)}\right)^2$

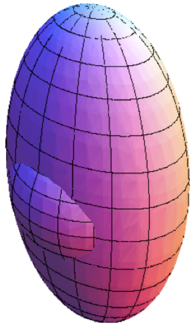

# Triaxial Rotor - classical

Angular momentum vector **R** with respect to the axes of the triaxial nucleus

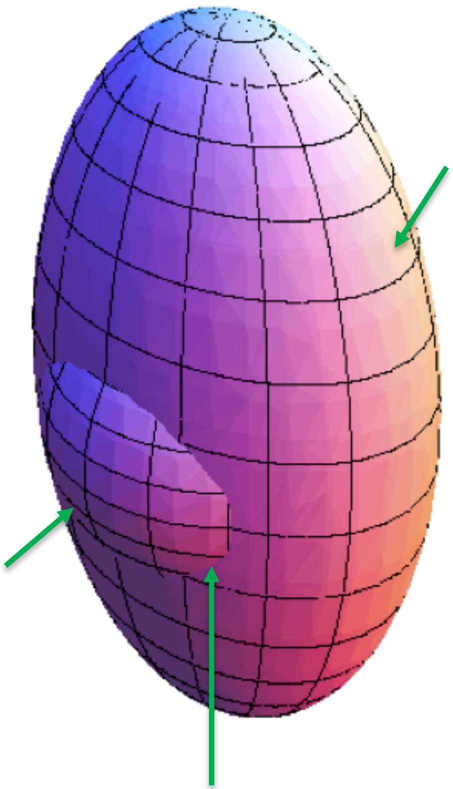

Energy conserved

Angular momentum conserved

Classical orbit

# Terminology:

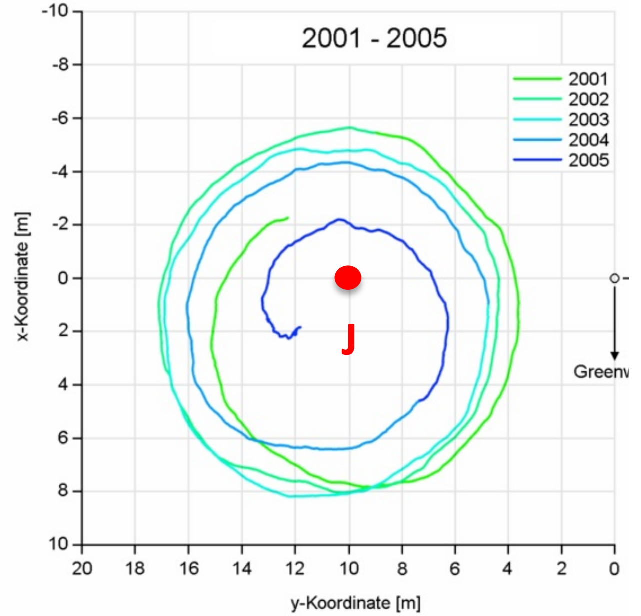


Bohr and Mottelson
introduced ``wobbling" in Nuclear Structure II, p.190 ff.
They describe the mode as
`”… *the precessional motion of the axes with respect to the direction of I; for small amplitudes this motion has the character of a harmonic vibration …”*

wobbling of the rotation axis of the earth

-Specify the mode by the axis that the angular momentum vector revolves in the body fixed frame.

medium axis wobbling: W-m

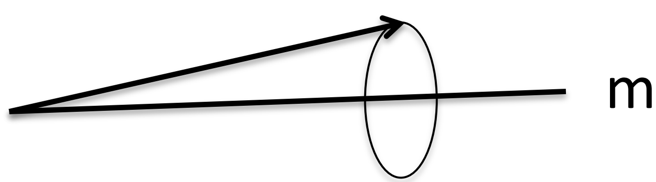

Triaxiality enables collective rotation about all three principal axes.
Classification of the TR States be based on
correspondence with classical orbit.

$$H_{TR} = \frac{R_s^2}{2\Im_s} + \frac{R_m^2}{2\Im_m} + \frac{R_l^2}{2\Im_l}, \quad \Im_m > \Im_s > \Im_l \text{ irrotational, quantal order}$$

$$R^2 = R_s^2 + R_m^2 + R_l^2$$

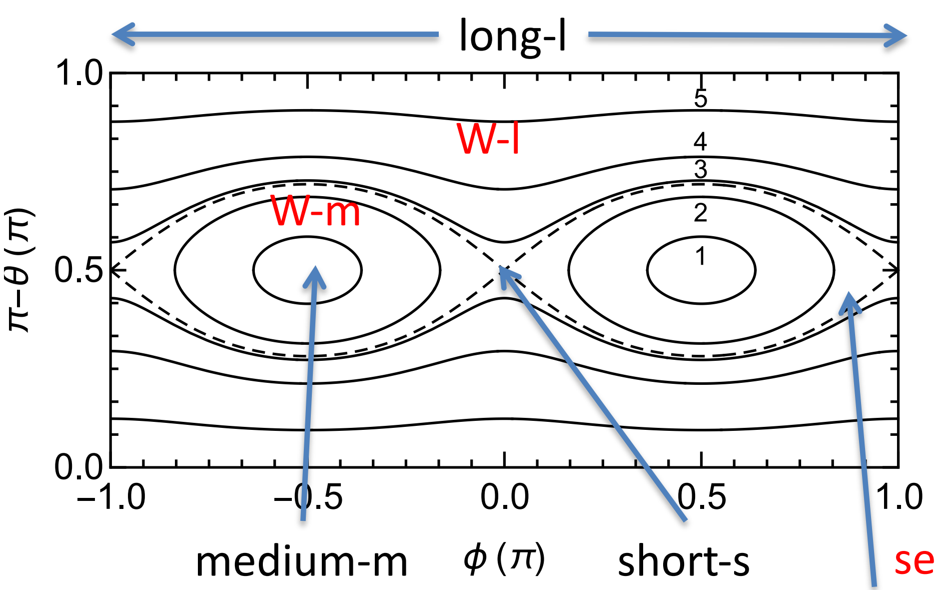


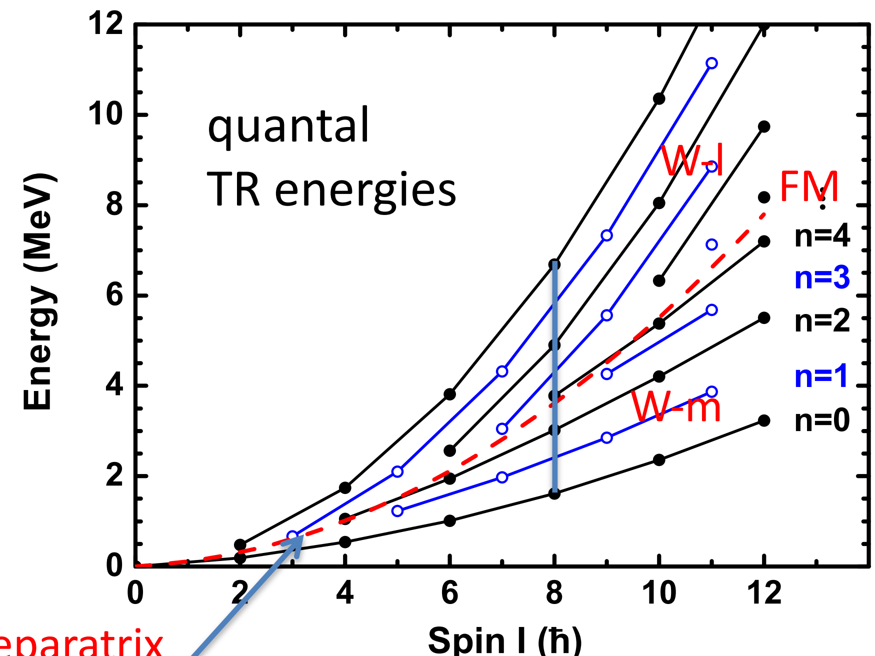


separatrix
flip-mode FM

classical orbits ($R$=8)
have distinct topology separated by
------ separatrix

$$\Im_m = 30\frac{\hbar^2}{MeV}, \Im_m = 10\frac{\hbar^2}{MeV}, \Im_l = 5\frac{\hbar^2}{MeV}.$$

# *Classical orbits*

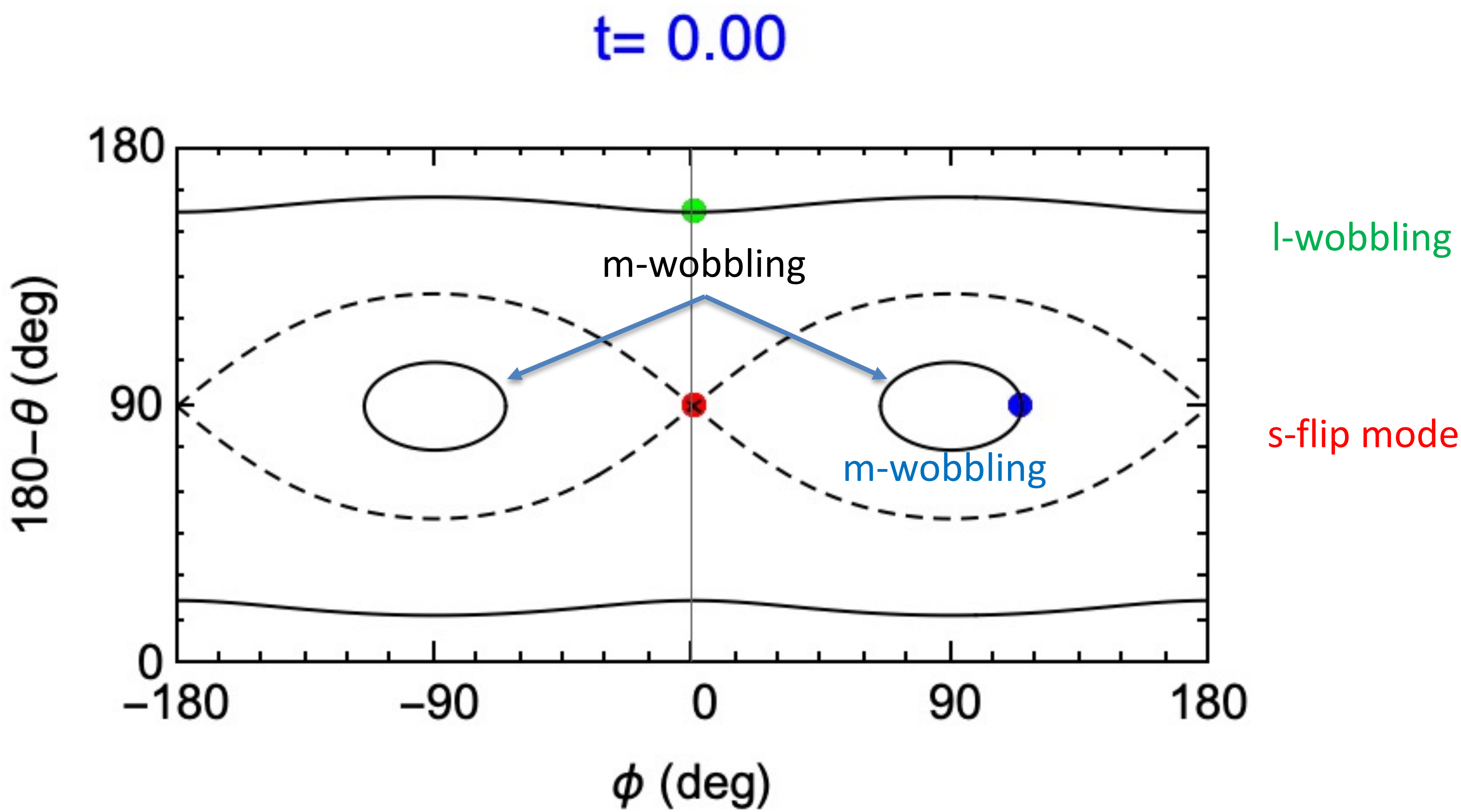


**Precession with respect to the principal axes.**

E. A. Lawrie ,1,2,* O. Shirinda ,1,† and C. M. Petrache 3, PHYSICAL REVIEW C 101, 034306 (2020)

New terminology: Tilted precession – TiP is the same as "Wobbling " in the original Bohr Mottelson definition

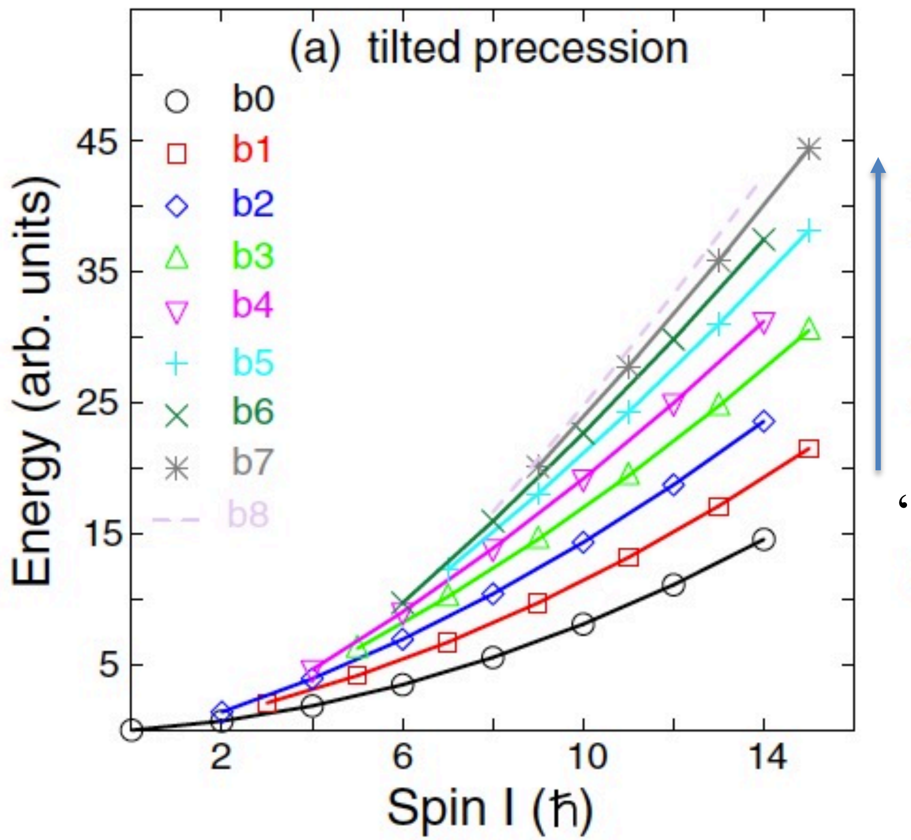


Increasing component transverse to m-axis

"Wobbling" only if equidistant

Keep it simple! The original "Wobbling" is appropriate.

See Q. B. Chen's talk for more concerning the particle-rotor system

# An instructive representation: Spin Coherent State maps

Re-express TR state in the continuous non-orthogonal normalized basis of

**Spin Coherent States (SCS)** ,

which are generated by rotating the state of maximal projection on the *l*-axis $|RRK = R>$.

$$|\theta\phi>= e^{-i\hat{R}_l\phi}e^{-i\hat{R}_m\theta} \ |RRR>= \sum_K D^R_{RK}(0,\theta,\phi)|RRK>$$

Classical expectation values:

$$<\theta\phi|\hat{R}_l|\theta\phi>= R\cos\theta, \quad <\theta\phi|\hat{R}_s|\theta\phi>= R\sin\theta\cos\phi, \quad <\theta\phi|\hat{R}_s|\theta\phi>= R\sin\theta\sin\phi$$

Finite widths: $\Delta\hat{R}_i = \sqrt{<\theta\phi|\hat{R}_i^2|\theta\phi>-<\theta\phi|\hat{R}_i|\theta\phi>^2} \approx \sqrt{2R}$

corresponding to an angle uncertainty: $\Delta\theta \approx \Delta\phi \approx 1/\sqrt{2R}$

**SCS maps** of TR states: probability distributions of the SCS basis states

$$P(\theta,\phi) = \frac{2R+1}{4\pi}\sin\theta\sum_{KK'}\rho^{(\nu)}_{KK'}D^{R*}_{RK}(0,\theta,\phi)D^R_{RK}(0,\theta,\phi),$$

density matrix: $\rho^{(\nu)}_{KK'} = c^{(\nu)}_K c^{(\nu)}_{K'}$

$$\int d\theta\, d\phi P(\theta,\phi) = 1$$

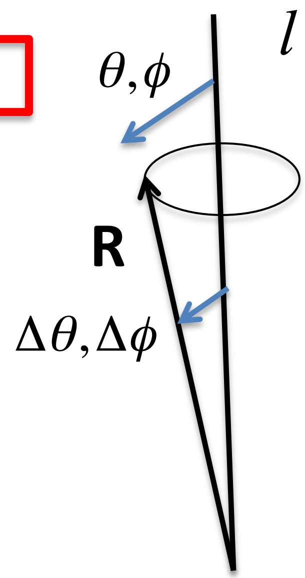

Spin Coherent State maps: Distilling the classical underpinning from quantal Triaxial Rotor states (TR)

-introduced/unpublished:
*S. Frauendorf, Chirality: from Symmetry to dynamics, Nordita workshop on Chiral bands in Nuclei, Stockholm, 20-22 April 2015, slides from talks,* https://www.nordita.org/events/workshops/list_of_workshops/index.php (2015)

-published:
Q. B. Chen & S.Frauendorf, EPJA 58 (2022) 58:75

-introduced as "azimuthal plots":
F.Q. Chen, Q.B. Chen, Y.A. Luo, J. Meng, S.Q. Zhang, Phys. Rev. C **96**, 051303(R) (2017)
and used in a number of later papers

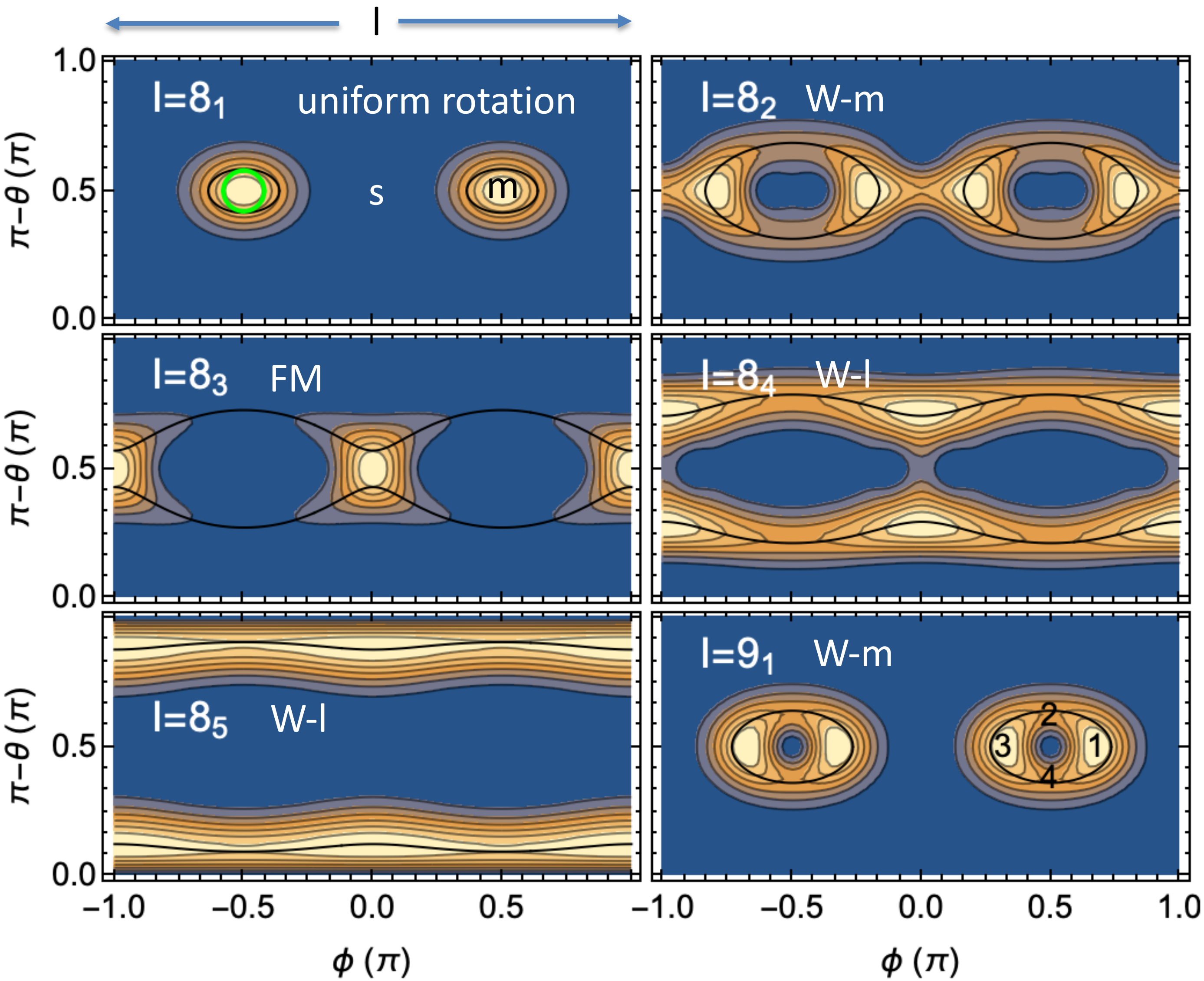


Classical orbits ←→ fuzzy rims

green circle: width of the SCS cones

# Even-even nuclei that classify as triaxial rotors are rare.

Static triaxiality according to staggering of the $\gamma$ band:
Odd-I-down relative to the even-I neighbors or
Even-I-up relative to the odd-I neighbors $\overline{S(6)}$>0.015
Most nuclei have $\overline{S(6)}$ <0.015: axial or $\gamma$ soft.

$$S(I) = \frac{E(I) - 2E(I-1) - E(I-2)}{E(2_1^+)}, \qquad \overline{S(I)} = \frac{S(I) - S(I+1)}{2}$$

| | $\overline{S(6)}$ | $\frac{E(2_2^+)}{E(4_1^+)}$ | |
|---|---|---|---|
| $^{76}$Ge | 0.12 | 0.78 | |
| $^{112}$Ru | 0.31 | 1.10 | good fit with $\gamma = 19^0$ and hydrodynamical MoI |
| $^{114}$Ru | 0.31 | 0.98 | |
| $^{114}$Pd | 0.13 | 1.15 | |
| $^{170}$Er | 0.42 | 3.59 | no, axial |
| $^{192}$Os | 0.37 | 0.84 | |
| $^{192}$Pt | 0.39 | 0.78 | |
| $^{232}$Th | 0.22 | 4.61 | no, axial |

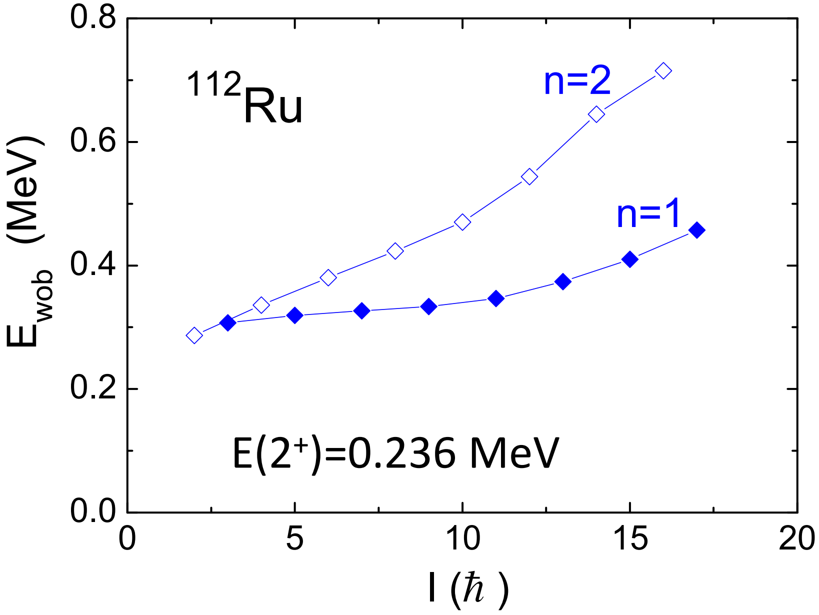


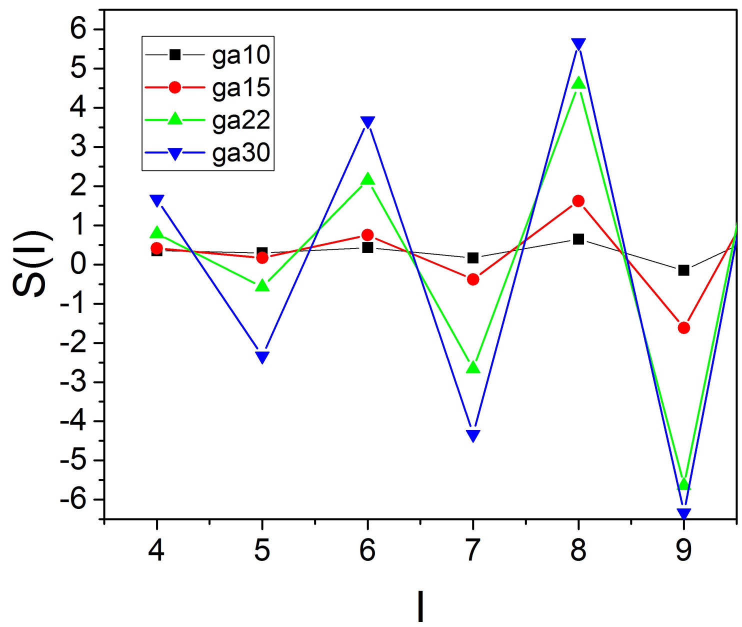


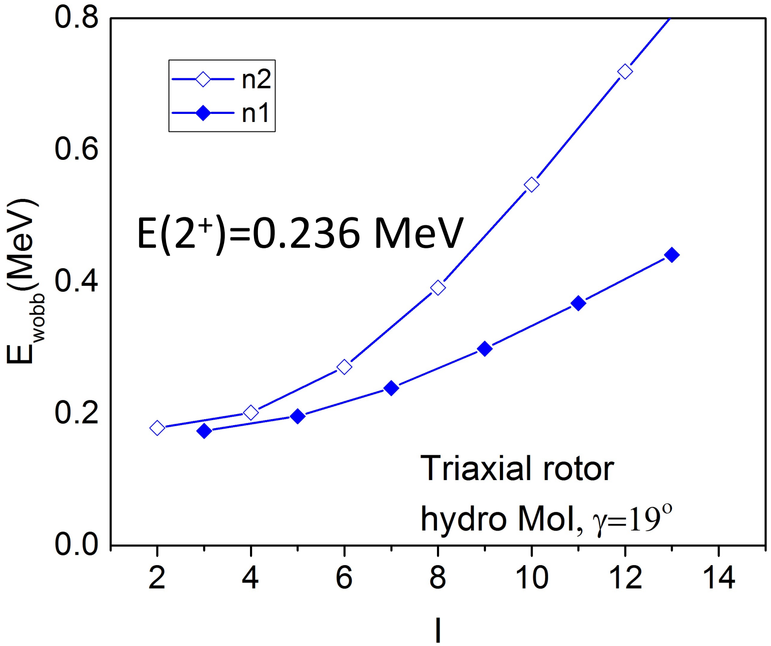


# The best e-e wobbler

# One particle (or one hole) + Triaxial Rotor

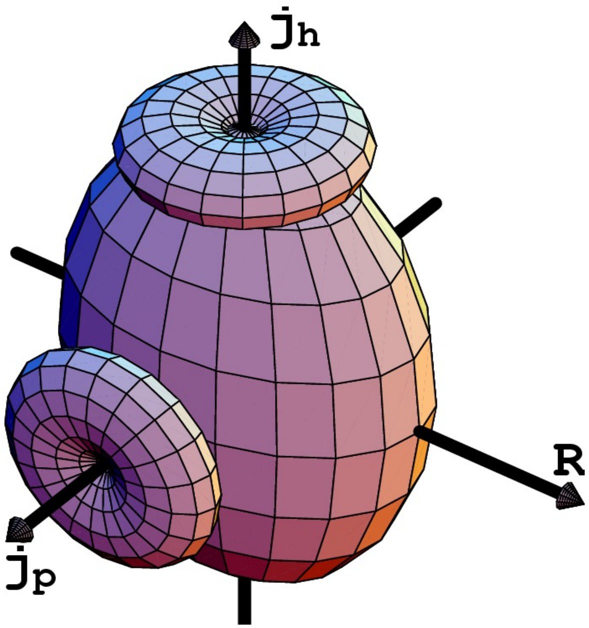


High-j orbitals:

$f_{7/2}$, $g_{9/2}$, $h_{11/2}$, $i_{13/2}$, $j_{15/2}$
particles tend to align their **j** with the s-axis,

$f_{7/2}$, $g_{9/2}$, $h_{11/2}$, $i_{13/2}$, $j_{15/2}$
holes tend to align their **j** with the l-axis,

# Particle Triaxial Rotor model (PTR)

$H_{PTR} = h_p + \frac{\hat{R}_s^2}{2\Im_s} + \frac{\hat{R}_m^2}{2\Im_m} + \frac{\hat{R}_l^2}{2\Im_l},\ \hat{R}_i^2 = (\hat{J}_i - \hat{j}_i)^2$, coupling to the triaxial potential $h_p(\hat{j}_i)$

is diagonalized in the discrete basis $|IIKk>=|IIK>|jk>$

of good total angular momentum $I$, projection $I$ on the z-lab axis

with projection $K$ on the $l$- body axis, $-I \le K \le I$, and

of good particle angular momentum j with projection k on the $l$- body axis, $-j \le k \le j$,

PTR eigenstates: $|II\nu>=\frac{1}{\sqrt{2}}\sum_{Kk} c_{Kk}^{(\nu)} |IIKk>$, $K-k$ even, $c_{-K-k}^{(\nu)} = (-)^{I-k} c_{Kk}^{(\nu)}$

represented by the discrete probability amplitudes $<IIKk|II\nu>=c_{Kk}^{(\nu)}$

Deformation parameters $\varepsilon, \gamma$ are input parameters.
They control how strongly the particles are coupled to the triaxial core.
Taken from mean field calculations for the non-rotating particle+core system.

Core moments of inertia are further input parameters.
They control the inertial forces.

Quantum mechanic requires that $\Im_i = 0$ if $i$ is a symmetry axis.

Excludes rigid body ratios of $\Im_i$.

Irrotational flow ratios $\Im_i \propto \sin^2(\gamma - \frac{2i\pi}{3})$ obeys the symmetry.

However the ratios may deviate from the irrotational-flow ones.

The stronger pairing the closer the $\Im_i$ approach the irrotational values.

For realistic pairing deviations are expected -> freedom to fit the ratios.

(See e.g. Ratios between $\Im_i$ of e-e system by cranking model.
S. Frauendorf, PHYSICAL REVIEW C 97, 069801 (2018))

Pauli principle acting between the core and the valence particles (exchange terms) may further modify effective core MoI

$$\mathfrak{I}_m > \mathfrak{I}_s > \mathfrak{I}_l$$

strong E2, I->I-1,

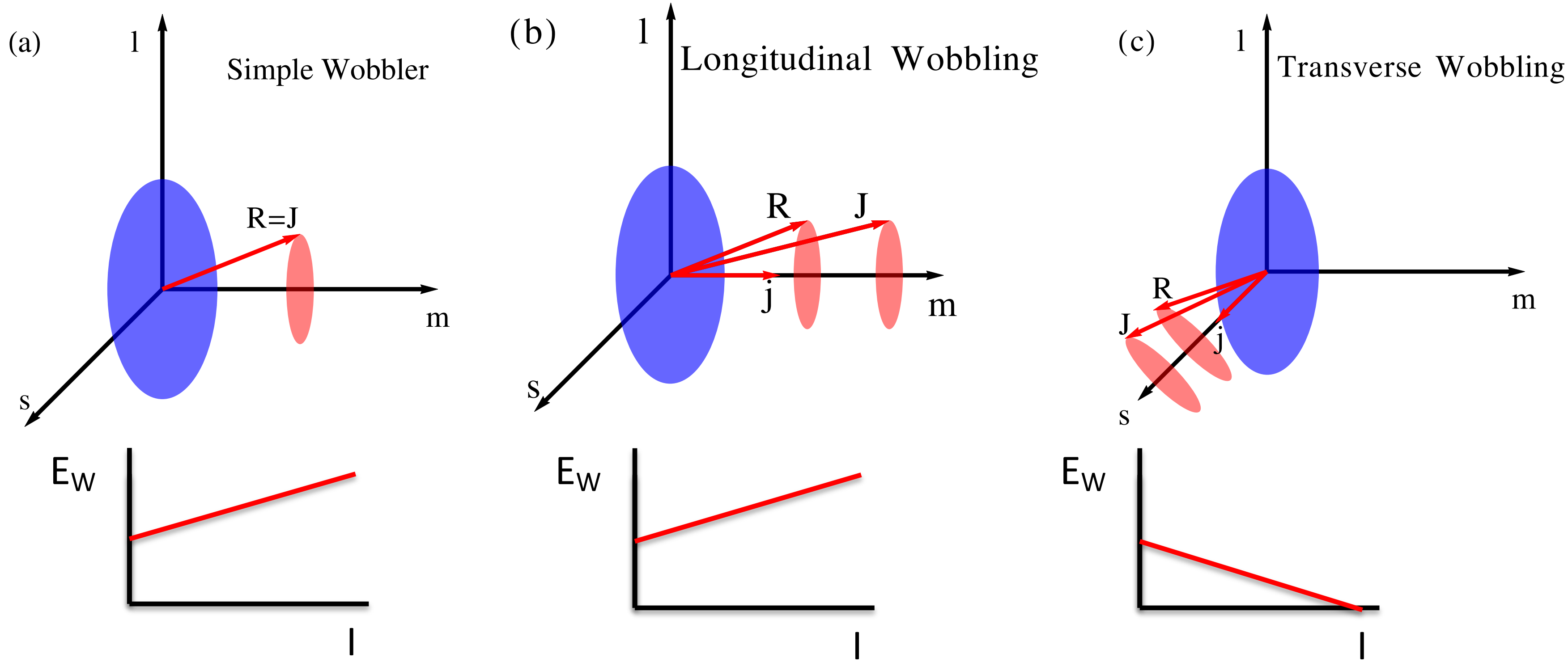


strong E2 I->I-1

wobbling and signature partner band classification Doenau, S. F., PRC 89(2014)

weak E2 I->I-1

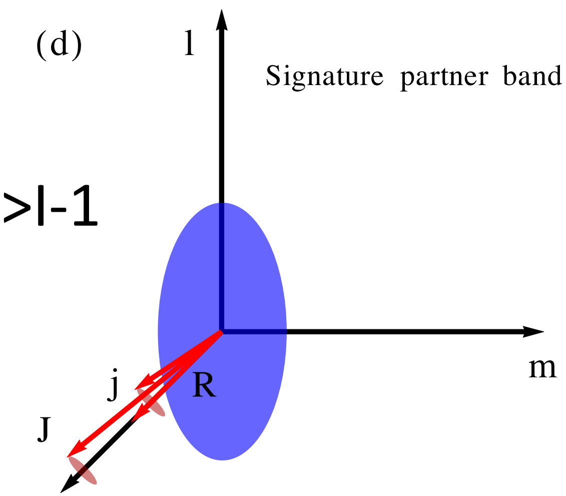

To account for the strong reaction of the valence particles to the inertial forces use the less restrictive topological classification by the orientation of the precession cone of **J**.

| | m-axis has maximal moment of inertia | |
|---|---|---|
| | Transverse Wobbling | Longitudinal Wobbling |
| topological<br>Q. B.Chen, S. F.<br>EPJA 75(2022) | total **J** revolves<br>around s- or l- axis | total **J** revolves<br>around m- axis |
| original<br>F. Doenau, S. F.<br>PRC 89(2014) | particle **j** aligned<br>with s- or l- axis<br>total **J** revolves<br>around s- or l- axis | particle **j** aligned<br>with m- axis<br>total **J** revolves<br>around m- axis |
| experimental | wobbling energy<br>decreases with I,<br>strong E2  I->I-1 | wobbling energy<br>increases with I,<br>strong E2  I->I-1 |

# Example $^{135}$Pr

Example

S. Frauendorf, F. Doenau, PRC 89 (2014) 014332

J. Matta et al. PRL 114, 082501 (2015),

N. Sensharma et al. PLB 792, 170 (2019)

QTR: one $h_{11/2}$ low-shell quasiproton + Triaxial rotor

| nucleus | $\epsilon$ | $\gamma(deg)$ | model | $\mathcal{J}_m$ | $\mathcal{J}_s$ | $\mathcal{J}_l$ |
|---|---|---|---|---|---|---|
| 135Pr | 0.16 | 26 | fit | 21 | 13 | 4 |

## Correspondence with classical orbits:

The TR is one dimensional in the R=const space.
→ One to one correspondence between classical orbit and quantum states.
The PTR is two, three, … dimensional in the J=const space.
To apply topological classification by correspondence
we introduce the adiabatic classical energy .

Minimize the classical PTR energy

$$E_{PTR}(\theta,\phi,\vartheta,\varphi) = h_p(j_i) + \frac{R_s^2}{2\Im_s} + \frac{R_m^2}{2\Im_m} + \frac{R_l^2}{2\Im_l},\ R_i^2 = (J_i - j_i)^2 \rightarrow E_{ad}(\theta,\phi)$$

with respect to orientation of the particle angular momentum $j_i(\vartheta,\varphi)$
for fixed orientation of total angular momentum $J_i(\theta,\phi)$.
Minimum of $E_{ad}(\theta,\phi)$ classical yrast line.
Setting $E_{ad}(\theta,\phi) = E_\nu \rightarrow$ the classical orbits corresponding to the PTR states.

# Classical adiabatic energy $E_{ad}(\theta,\phi)$

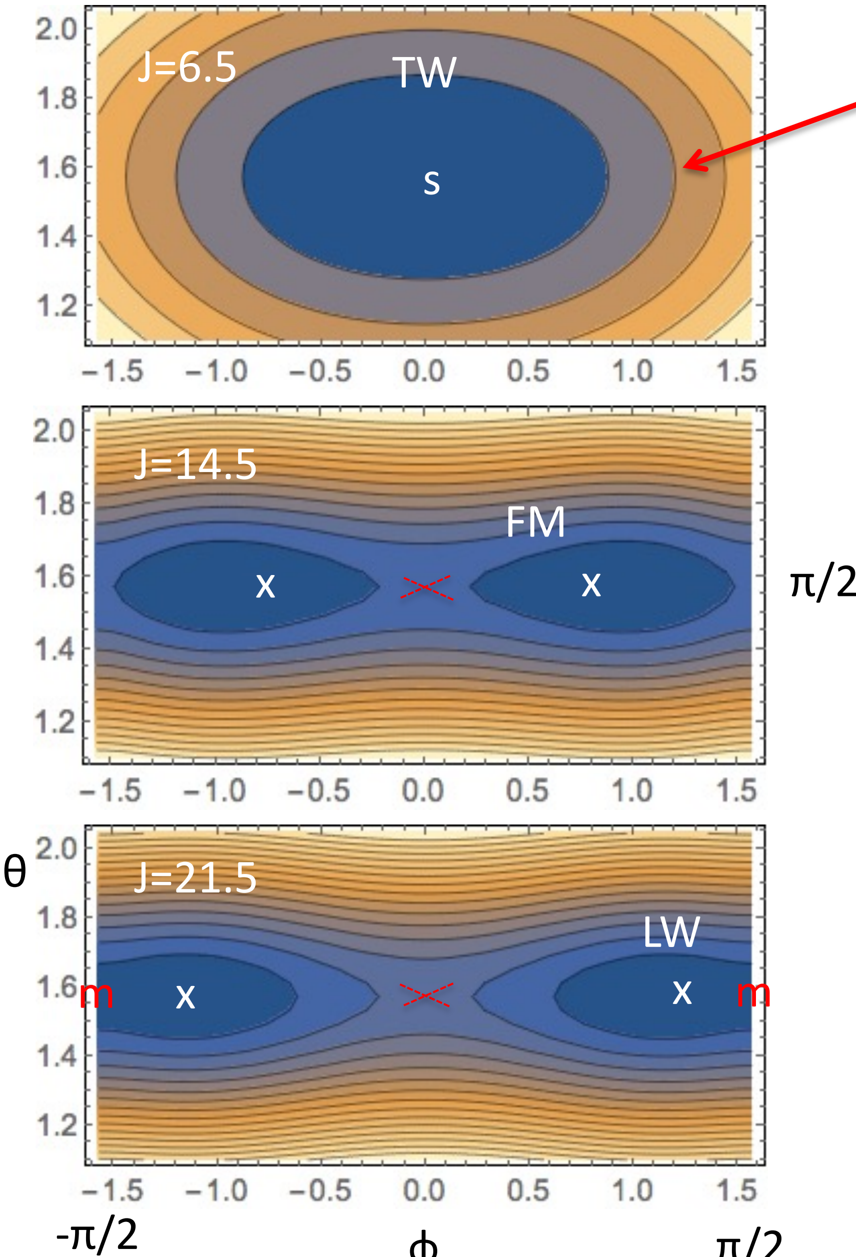


Classical adiabatic orbits

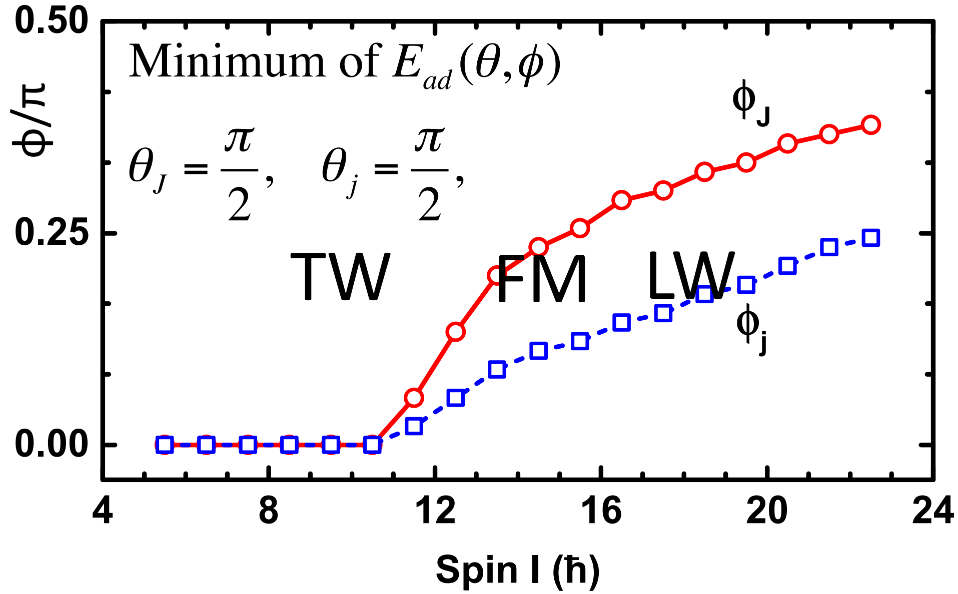


Transverse Wobbling TW

**J** revolves around the s-axis that is transverse to m-axis with the maximal moment of inertia

Flip Mode FM

Longitudinal Wobbling LW

**J** revolves around the m-axis with the maximal moment of inertia

# Distilling its classical underpinnings from a PTR state

**J - SCS maps** : total angular momentum probability distributions of the SCS basis states

$$P(\theta\phi)_{I\nu} = \frac{2I+1}{4\pi}\sin\theta\sum_{KK'}\rho^{(\nu)}_{KK'}\, D^{I*}_{IK}(0,\theta,\phi)D^{I}_{IK}(0,\theta,\phi),$$

density matrix: $\rho^{(\nu)}_{KK'} = \sum_{k} c^{(\nu)}_{Kk} c^{(\nu)}_{K'k}$

**j - SCS maps** : particle angular momentum probability distributions of the SCS basis states

$$P(\theta\phi)_{j\nu} = \frac{2j+1}{4\pi}\sin\theta\sum_{KK'}\rho^{(\nu)}_{kk'}\, D^{j*}_{jk}(0,\theta,\phi)D^{j}_{jk'}(0,\theta,\phi),$$

density matrix: $\rho^{(\nu)}_{kk'} = \sum_{K} c^{(\nu)}_{Kk} c^{(\nu)}_{Kk'}$

**R - SCS maps** : rotor angular momentum probability distributions of the SCS basis states

$$P(\theta\phi)_{R\nu} = \sin\theta\sum_{RK_RK_R'}\frac{2R+1}{4\pi}\rho^{(\nu)}_{R,K_RK_R'}\, D^{R*}_{RK_R}(0,\theta,\phi)D^{R}_{RK_R'}(0,\theta,\phi),$$

density matrix: $\rho^{(\nu)}_{R,K_RK_R'}$ in weak coupling basis $|IIKk> \rightarrow |IIjRK_R>$

# TW regime n=0, 1: **J** revolves around the s-axis

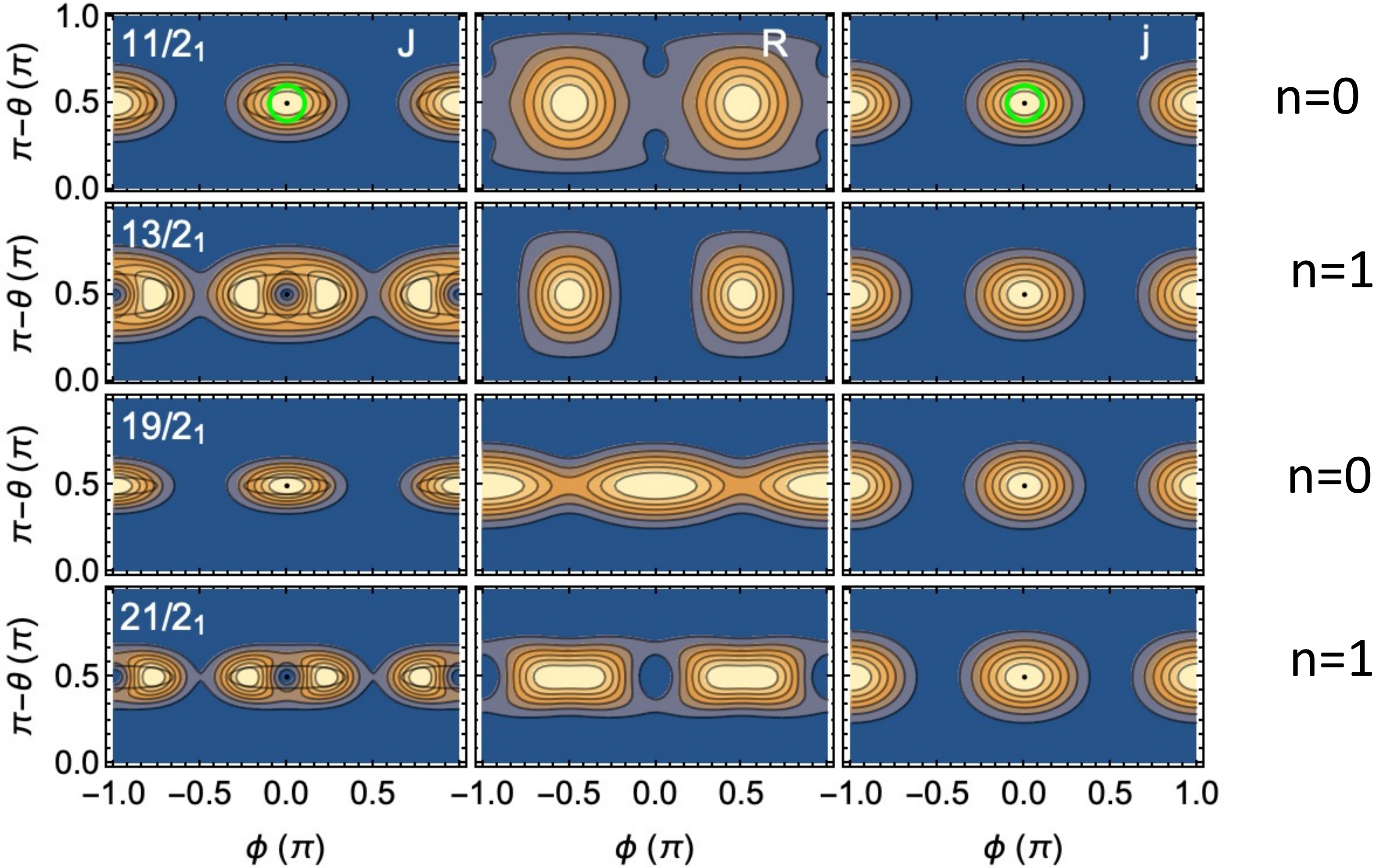


**j** stays close to the s-axis -> original definition of TW

$13/2_1$: **J** precession harmonic, $21/2_1$: unharmonic

# TW regime higher excitations

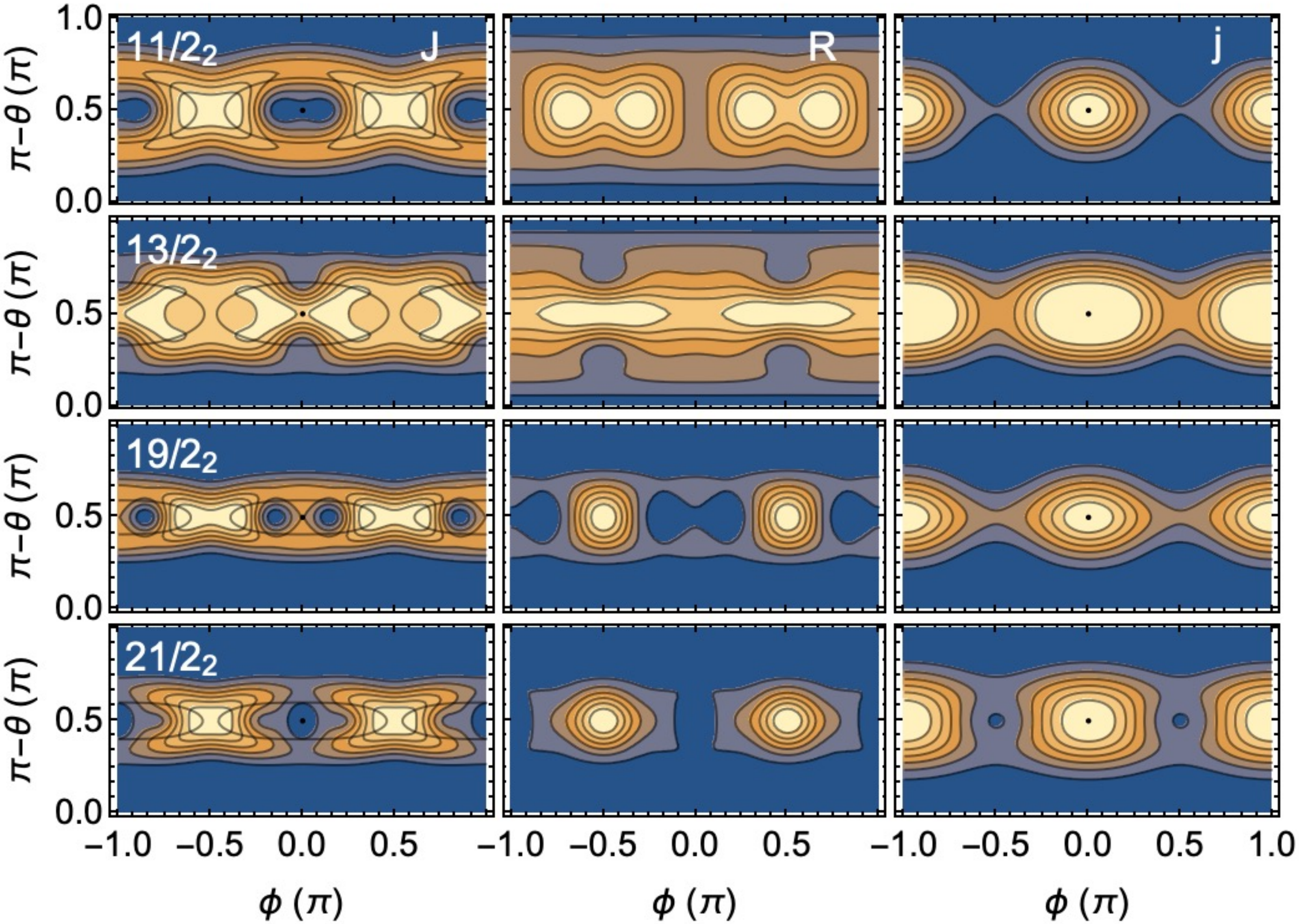


n=2

mixed

n=2

flip

$11/2_2$, $19/2_2$: **J** has still n=2 TW topology, highly perturbed,
**j** somewhat dealigned,
$13/2_2$, $21/2_2$: different from n=3 TW topology

# Transitional Flip regime

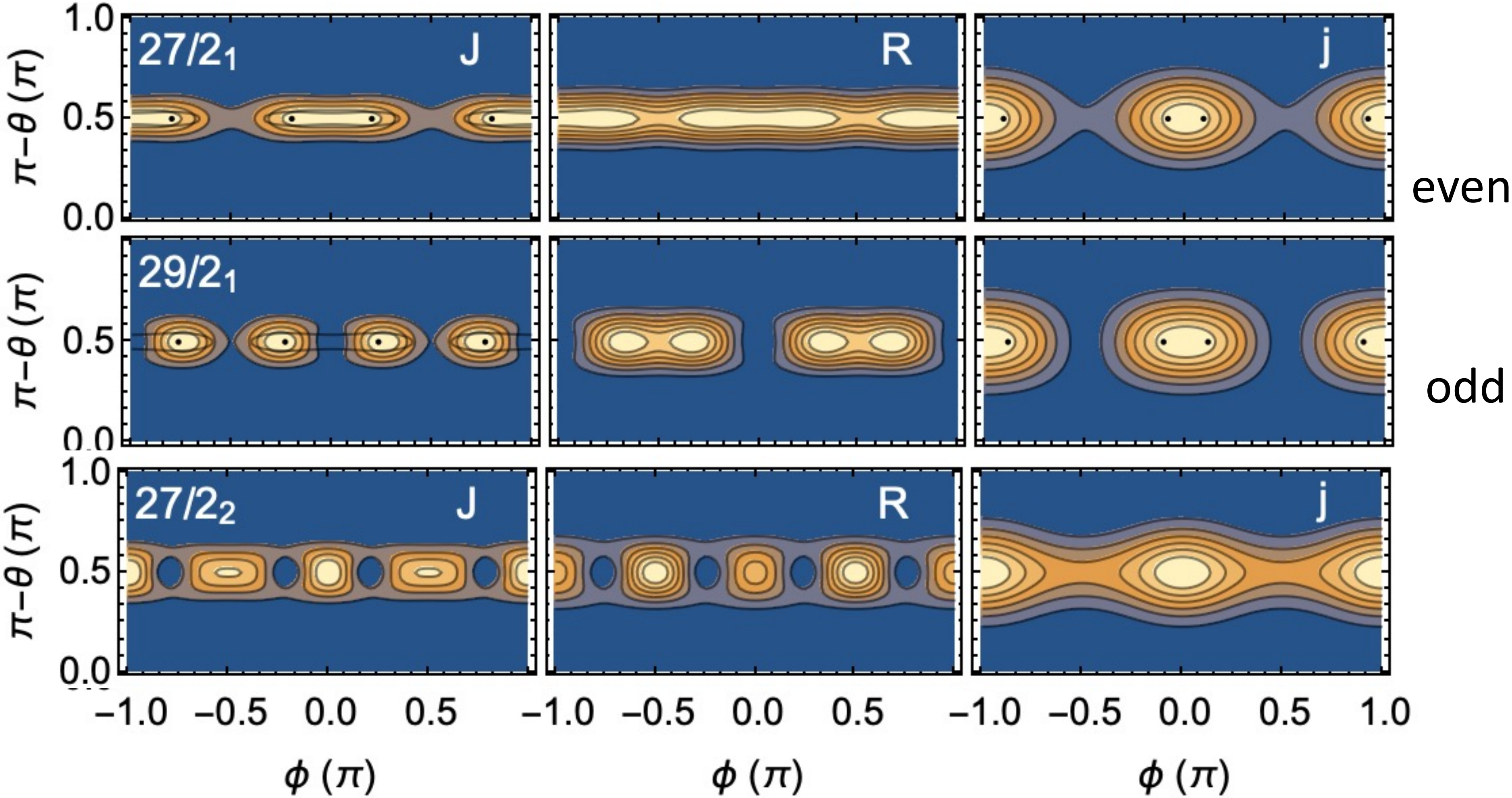


$27/2_1$ , $29/2_1$ : even and odd combinations of states localized at the classical energy minimum indicated by the dots -> FM signature restored branches of tilted axis rotation

$27/2_2$ : FM between the saddle points of the classical energy

LW regime

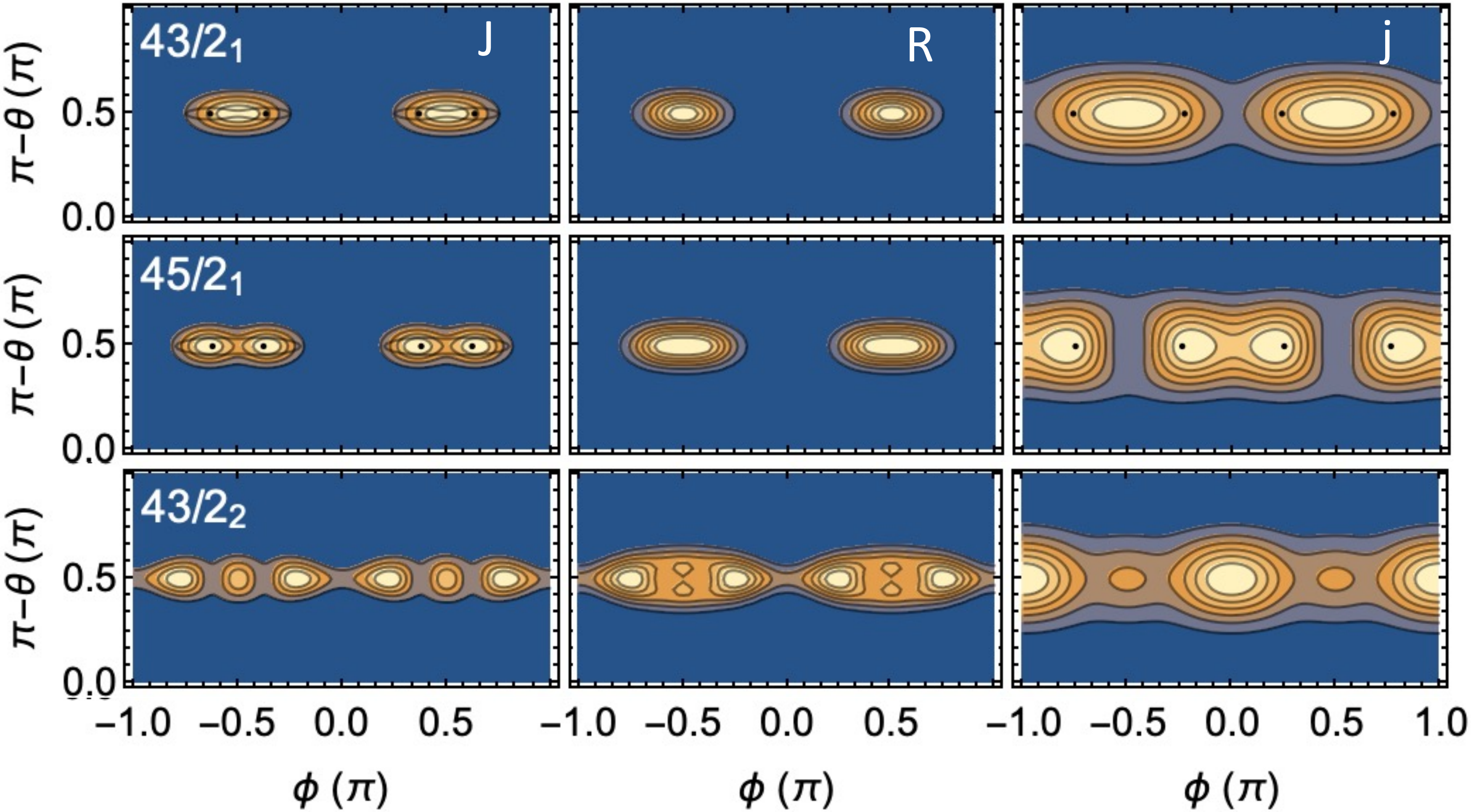


**J** revolves around the m-axis in a squeezed cone.

**J**, **R**, **j** are entangled.

$43/2_1$, $45/2_{1,}$ $43/2_2$: the $\phi_J$ distributions look like the ones of the n=0, 1, 2 states of a harmonic oscillator.

# TW regime  signature partner band

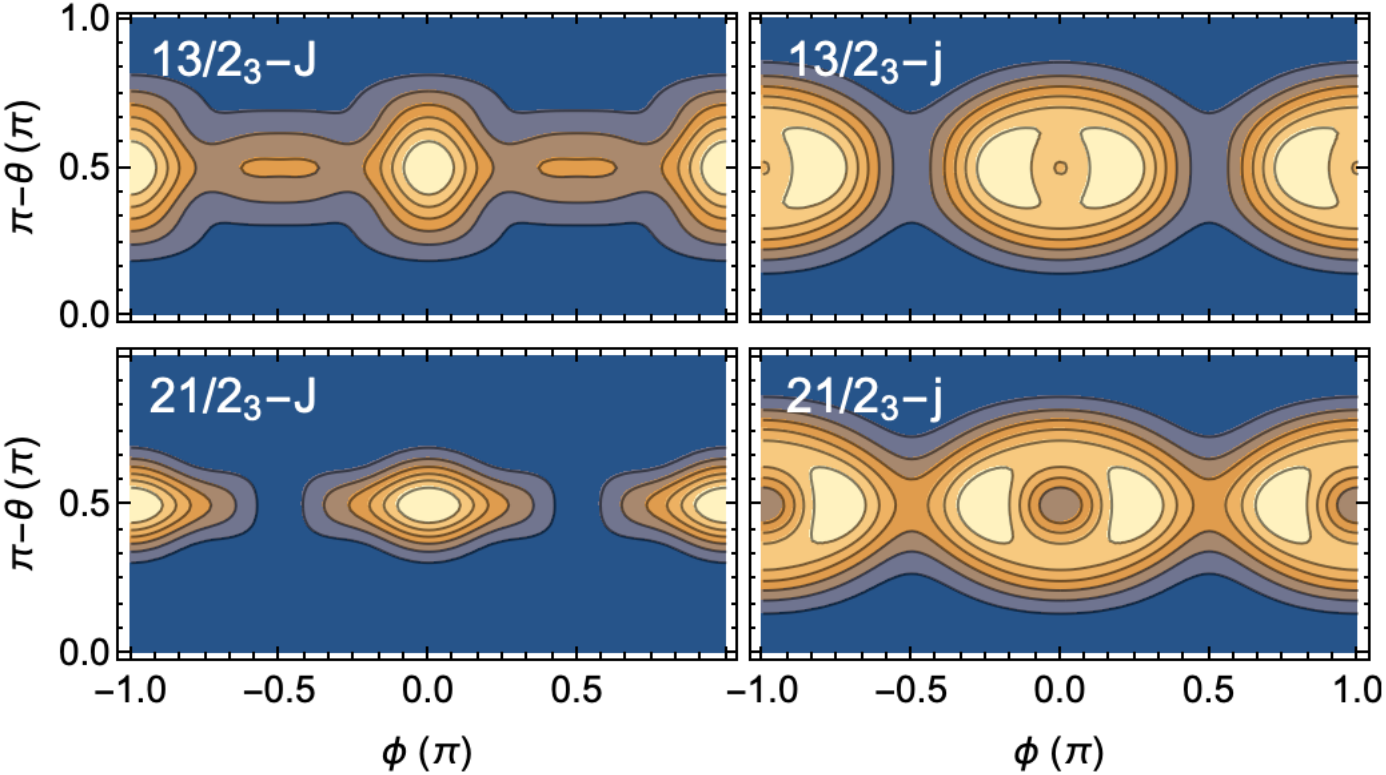


**J** rotates about the s- axis, **j** precesses around the s-axis
$13/2_3$ some admixture from TW n=2 state $13/2_3$

$$\mathfrak{I}_m > \mathfrak{I}_s > \mathfrak{I}_l$$

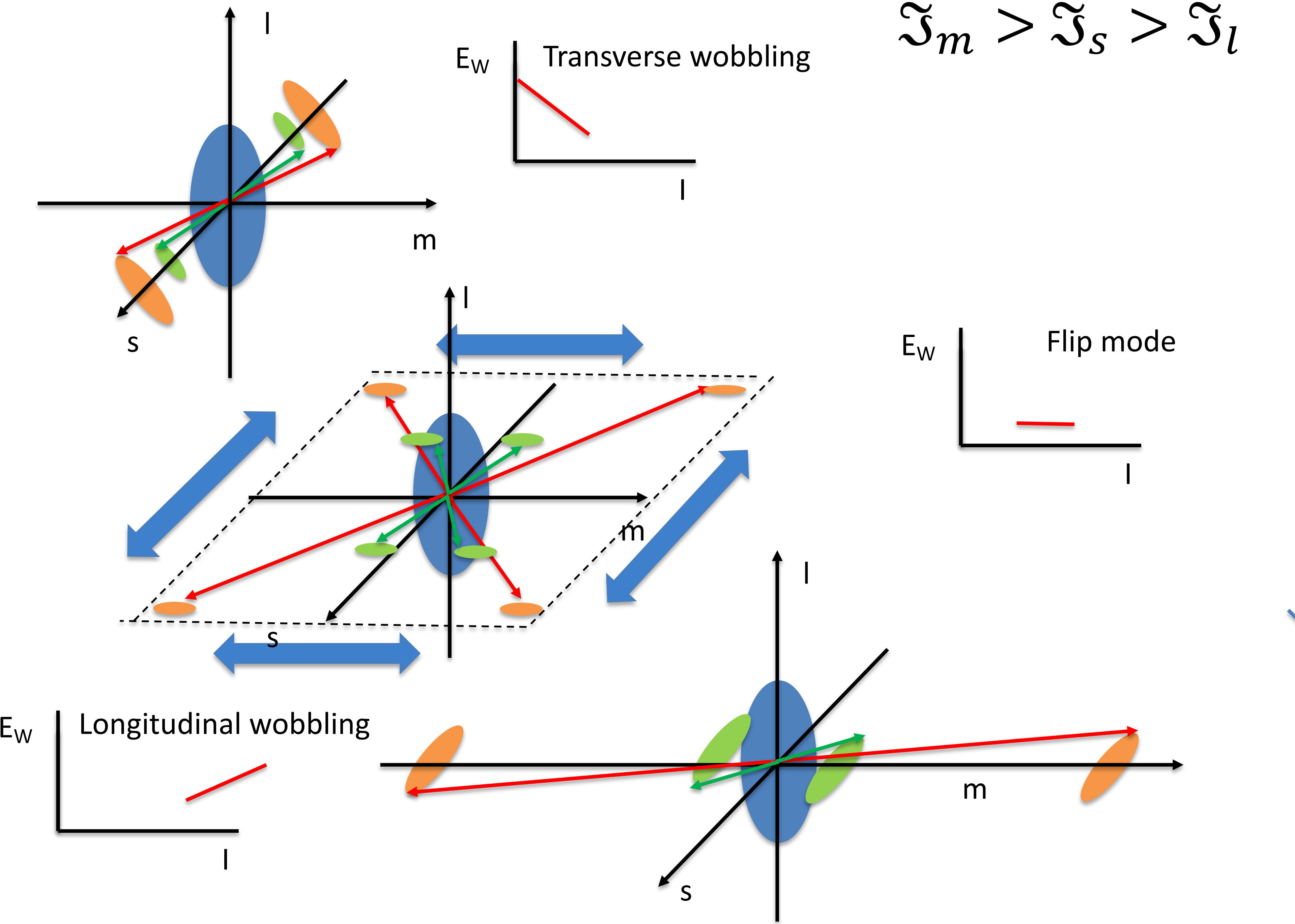

J. Matta et al. PRL 114, 082501 (2015), N. Sensharma et al. PLB 792, 170 (2019) experiment and

QTR: one $h_{11/2}$ low-shell quasiproton + Triaxial rotor interpretation

TPSM: Triaxial projected shell model interpretation

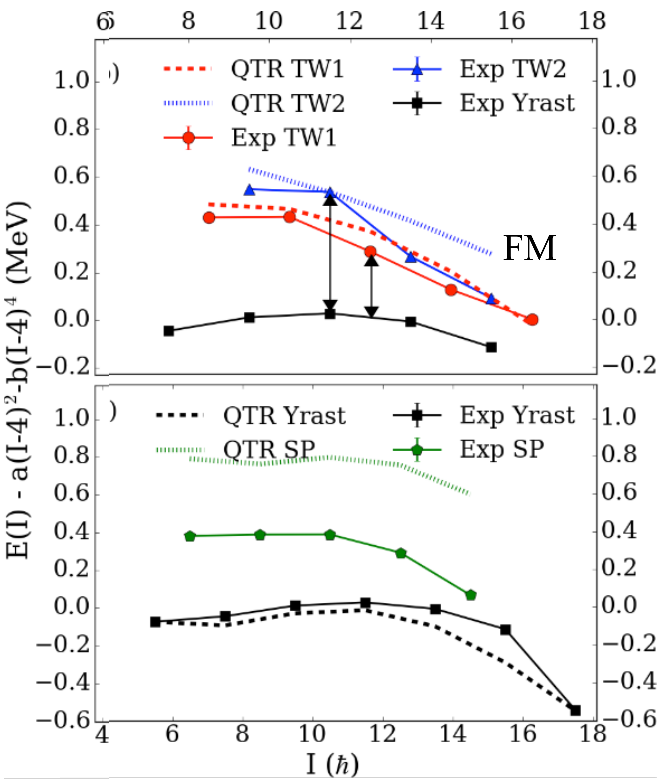


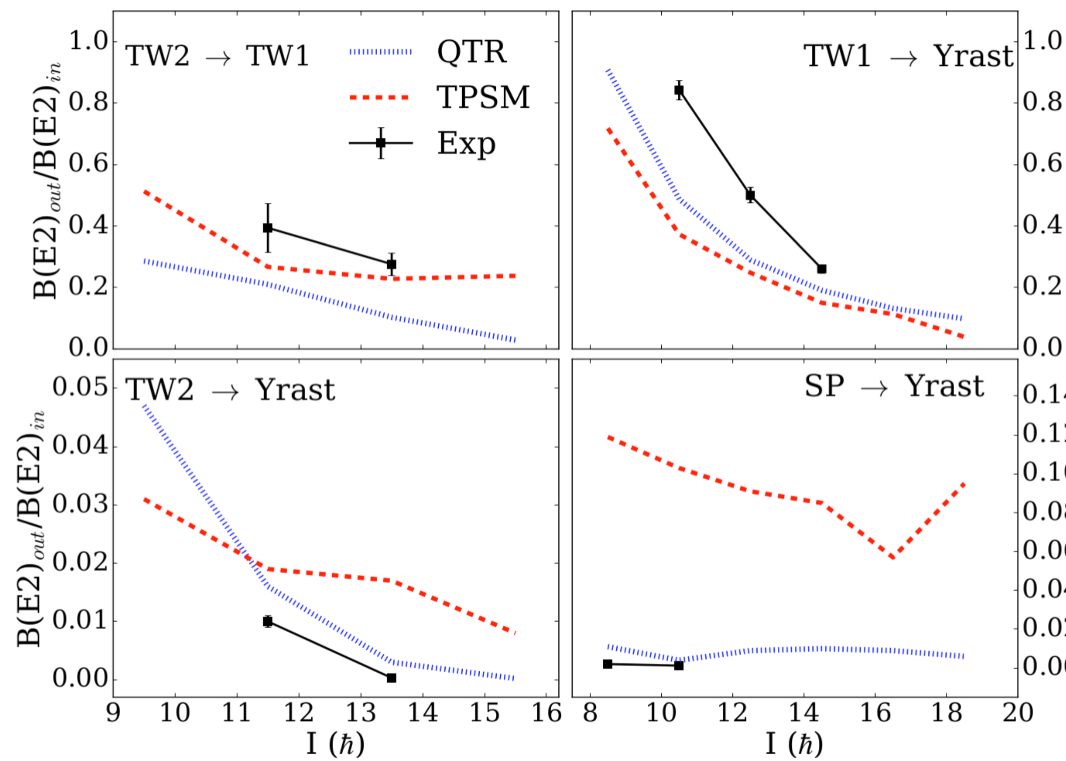


yrast: zero-phonon TW band

TW1: unharmonic one-phonon TW band

TW2: highly unharmonic two-phonon TW band

SP: unfavored signature band

QTR vs. PTR:

Inclusion of pairing enhances unharmonicities

# Evidence against the wobbling nature of low-spin bands in $^{135}$Pr , B. F. Lv et al., PLB 824 (2022) 13684

**Table 1**
The experimental polarization value $P$, angular correlation ratios $R_{ac}$, mixing ratios $\delta$, and ratios of out-of-band and in-band reduced transition probabilities of the connecting transitions between bands 3 and 1, and between bands 4 and 3.

| $E_\gamma$ (keV) | $P$ | $R_{ac}$ | $\delta$ | $\frac{B(M1)_{out}}{B(E2)_{in}}$ | $\frac{B(E2)_{out}}{B(E2)_{in}}$ |
|---|---|---|---|---|---|
| 747.3 | $0.04^{+8}_{-13}$ | 0.37(4) | $-0.47^{+9}_{-22}$ | | |
| 813.2 | $-0.03^{+5}_{-12}$ | 0.48(6) | $-0.37^{+10}_{-14}$ | 0.4(3) | 0.12(8) |
| 755.1 | | 0.50(6) | | | |
| 450.2 | $-0.07^{+9}_{-10}$ | 0.49(4) | $-0.31^{+10}_{-13}$ | | |

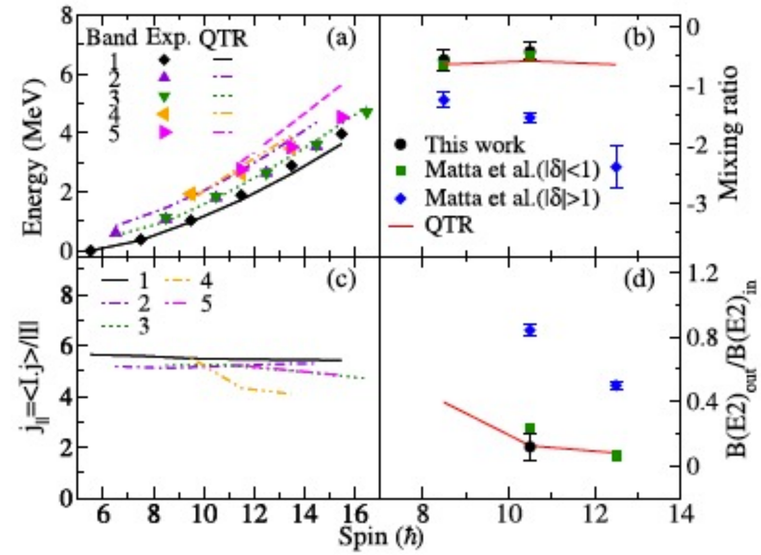


One proton + triaxial rotor $\varepsilon_2 = 0.16 \ \gamma = 26^o$

| nucleus | $\epsilon$ | $\gamma(deg)$ | model | $\mathcal{J}_m$ | $\mathcal{J}_s$ | $\mathcal{J}_l$ |
|---|---|---|---|---|---|---|
| 135Pr | 0.16 | 26 | fit | 21 | 13 | 4 |
| | 0.16 | 26 | hydrodyn | 20 | 6 | 4 |
| | 0.16 | 26 | cranking | 17 | 7 | 3 |

Strong parameter dependence:
Fitted MoI give transverse wobbling.
Hydro MoI give longitudinal wobbling.

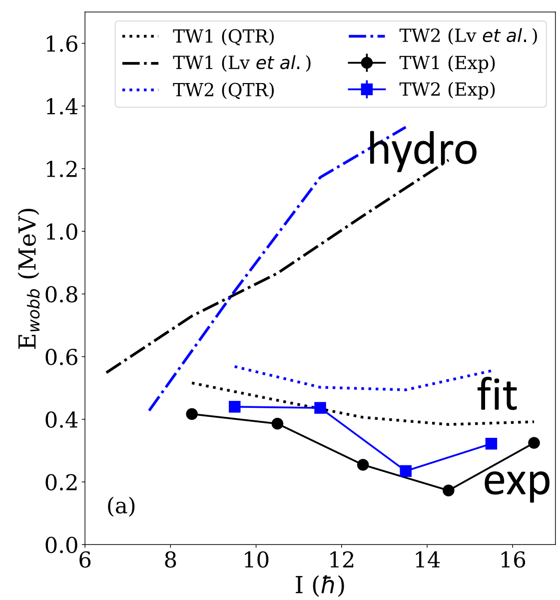

# $^{105}$Pd the mirror of $^{135}$Pr: $h_{11/2}$ proton replaced by a $h_{11/2}$ neutron

Favors the large-$|\delta|$ measurement for $^{135}$Pr.

PRM calculation with $\beta = 0.25, \gamma = 28^0$, hydro MoI gives transverse wobbling, $|\delta| \sim 2$

See Q. B Chen's talk

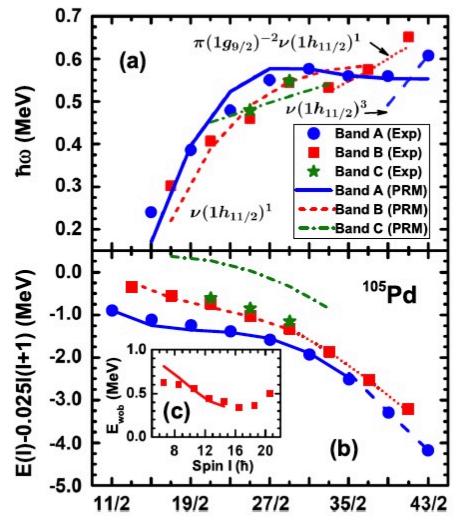


J. Timar et al, PHYSICAL REVIEW LETTERS **122,** 062501 (2019)

TABLE I. The experimental and theoretical multipole mixing ratios $\delta$ as well as the transition probability ratios $B(M1)_{\text{out}}/B(E2)_{\text{in}}$ and $B(E2)_{\text{out}}/B(E2)_{\text{in}}$ for the transitions from band $B$ to $A$ in $^{105}$Pd.

| | | $\delta$ | | $[B(M1)_{\text{out}}/B(E2)_{\text{in}}](\mu_N^2/e^2b^2)$ | | $[B(E2)_{\text{out}}/B(E2)_{\text{in}}]$ | |
|---|---|---|---|---|---|---|---|
| $I_i^\pi \to I_f^\pi$ | $E_\gamma$ (keV) | Expt | PRM | Expt | PRM | Expt | PRM |
| $17/2^- \to 15/2^-$ | 991 | $1.8 \pm 0.5$ | 2.38 | $0.162 \pm 0.097$ | 0.105 | $0.66 \pm 0.18$ | 0.736 |
| $21/2^- \to 19/2^-$ | 1034 | $2.3 \pm 0.3$ | 2.30 [a] | $0.089 \pm 0.026$ | 0.069 | $0.60 \pm 0.09$ | 0.465 |
| $25/2^- \to 23/2^-$ | 994 | $2.7 \pm 0.6$ | 1.99 | $0.029 \pm 0.016$ | 0.057 | $0.34 \pm 0.07$ | 0.329 |

[a]Normalization point, see text.

# The $^{187}$Au $h_{9/2}$ band: longitudinal wobbling (LW)
# N. Sensharma et al. PRL 124, 052501 (2020)

QTR calculation

$h_{9/2}$ quasiproton coupled to the triaxial potential $\beta$=0.23 , $\gamma$=23$^o$, somwhat below midshell

and the triaxial rotor with $\Im_m = 37.4\dfrac{\hbar^2}{MeV}, \Im_m = 13.8\dfrac{\hbar^2}{MeV}, \Im_l = 5.8\dfrac{\hbar^2}{MeV}$.

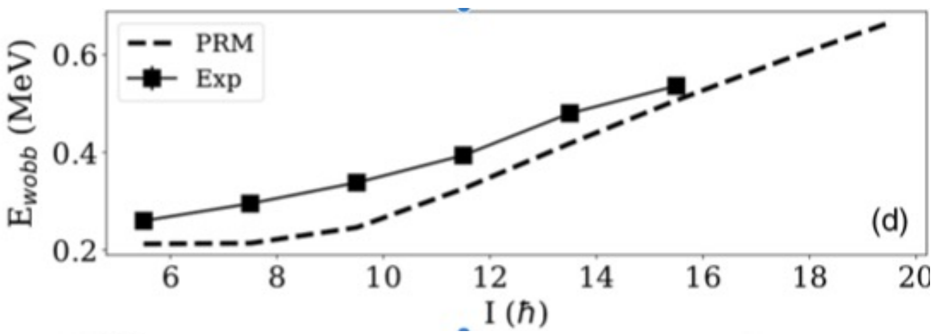


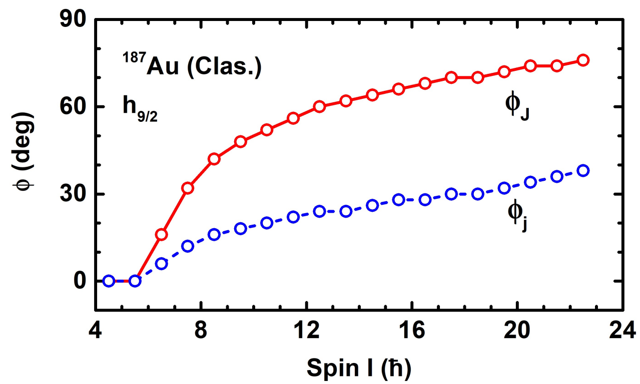


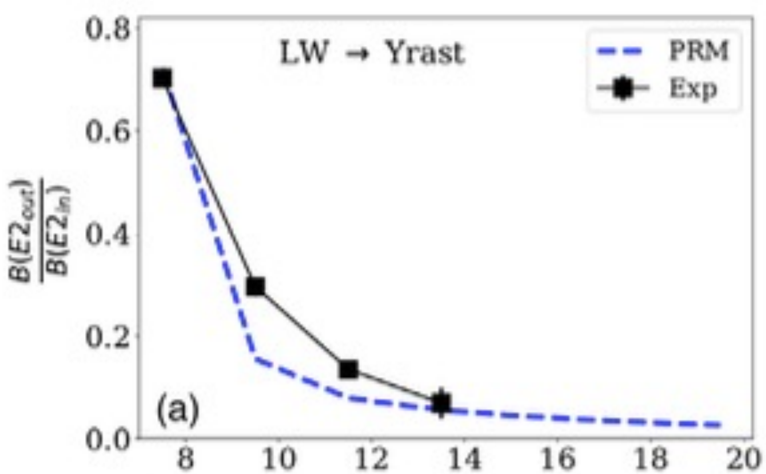


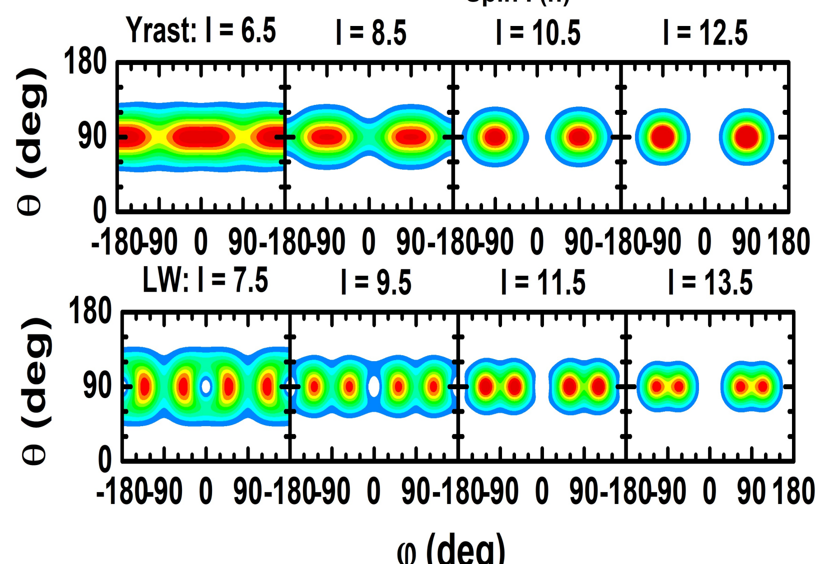

# Triaxial rotor + two $h_{11/2}$ neutrons

TABLE I. Experimental and theoretical mixing ratios $\delta$ as well as the transition probability ratios $B(M1)_{\mathrm{out}}/B(E2)_{\mathrm{in}}$ and $B(E2)_{\mathrm{out}}/B(E2)_{\mathrm{in}}$ for the transitions from band S1′ to band S1 of $^{130}$Ba.

| | $\delta$ | | $\frac{B(M1)_{\mathrm{out}}}{B(E2)_{\mathrm{in}}}\left(\frac{\mu_N^2}{e^2b^2}\right)$ | | $\frac{B(E2)_{\mathrm{out}}}{B(E2)_{\mathrm{in}}}$ | |
|---|---|---|---|---|---|---|
| $I$ ($\hbar$) | Expt | PRM | Expt | PRM | Expt | PRM |
| 13 | $-0.58^{+13}_{-13}$ | −0.67 | $0.36^{+19}_{-13}$ | 1.11 | $0.32^{+18}_{-15}$ | 0.51 |
| 15 | $-0.62^{+10}_{-10}$ | −0.68 | $0.38^{+61}_{-16}$ | 0.90 | $0.36^{+70}_{-19}$ | 0.42 |
| 17 | $-0.62^{+10}_{-10}$ | −0.68 | $0.23^{+22}_{-09}$ | 0.76 | $0.22^{+27}_{-10}$ | 0.35 |
| 19 | −0.60 | −0.66 | $0.25^{+23}_{-08}$ | 0.67 | $0.22^{+21}_{-07}$ | 0.29 |
| 21 | −0.60 | −0.63 | $0.43^{+35}_{-13}$ | 0.63 | $0.41^{+34}_{-13}$ | 0.25 |

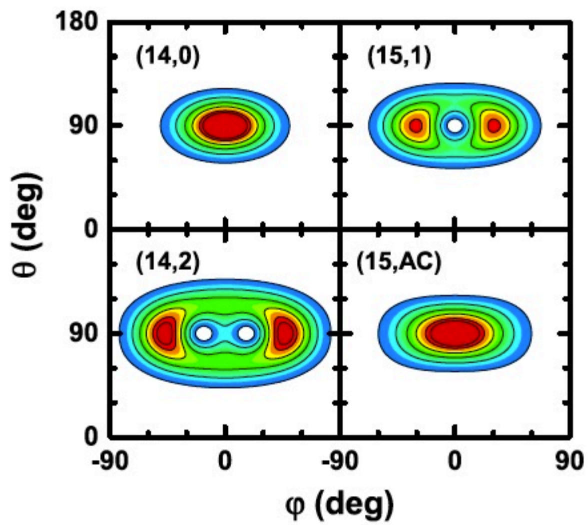


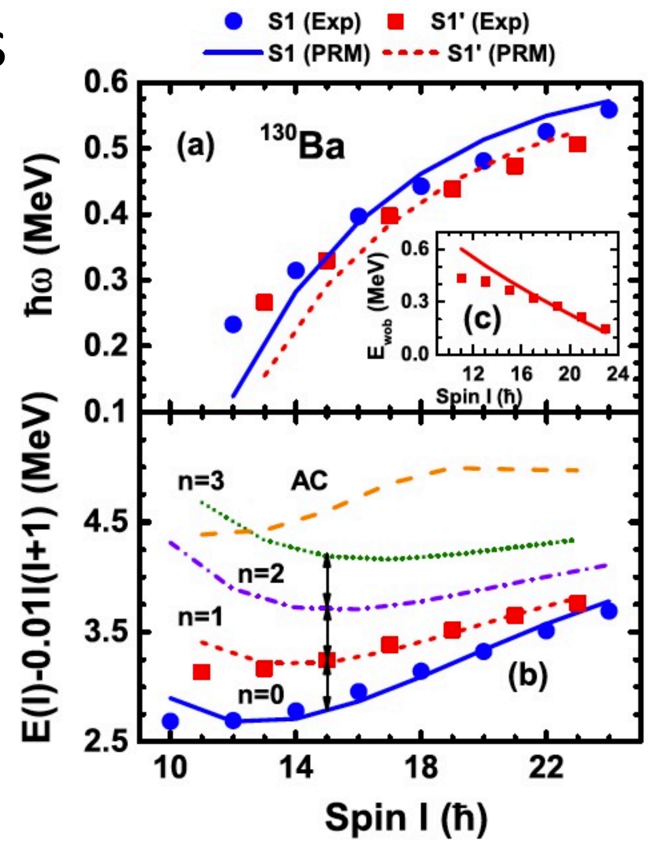


Transverse wobbling
Instability at I>22

**Transverse wobbling in an even-even nucleus**


Q. B. Chen[1,*] S. Frauendorf,[2,†] and C. M. Petrache[3,‡]



PHYSICAL REVIEW C **100**, 061301(R) (2019)

# $^{135}$Pr : ACM $^{134}$Ce as core

Weichuan Li, Thesis,University Notre Dame
and W. Li at al. Eur. Phys. J. A 58 (2022) 218

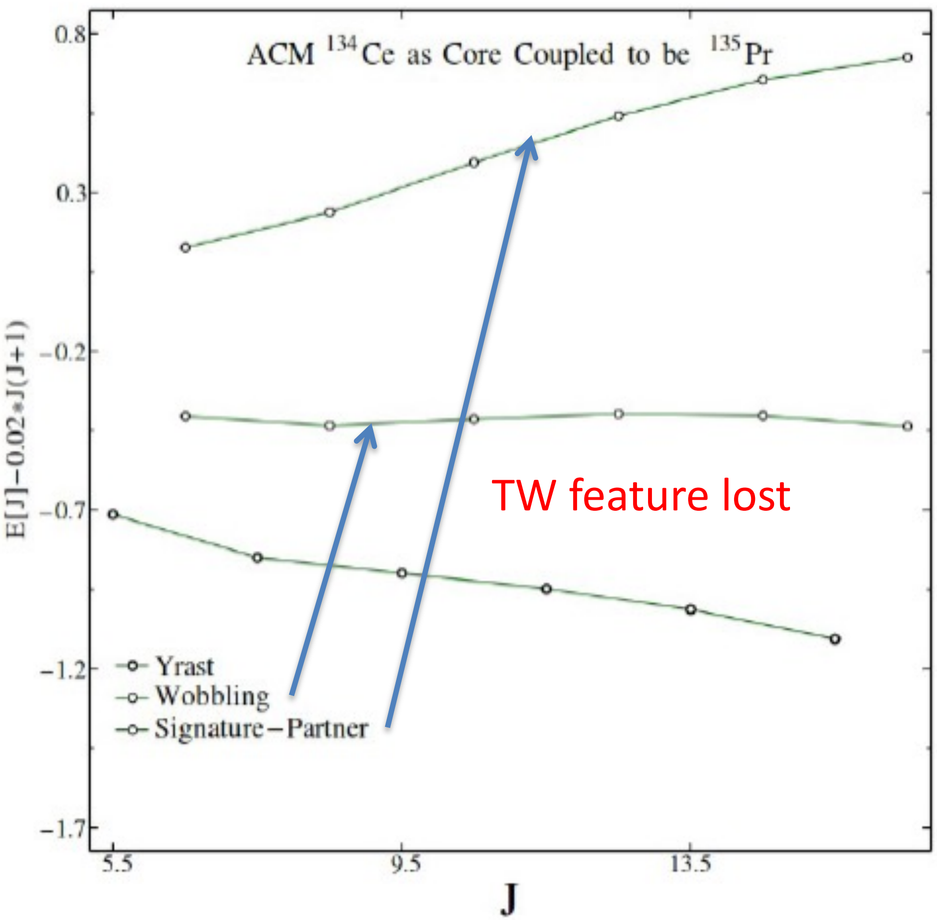


coupling to a "$\gamma$ soft core" ( Bohr Hamiltonian $H_B$)
by quasiparticle coupling model

$$H = h_{sph} + \kappa[qQ]_0 + \Delta P - \lambda N + H_B$$

Band(D): Quasi $\gamma$-band $^{134}$Ce

even-I-down pattern of $\gamma$ softness

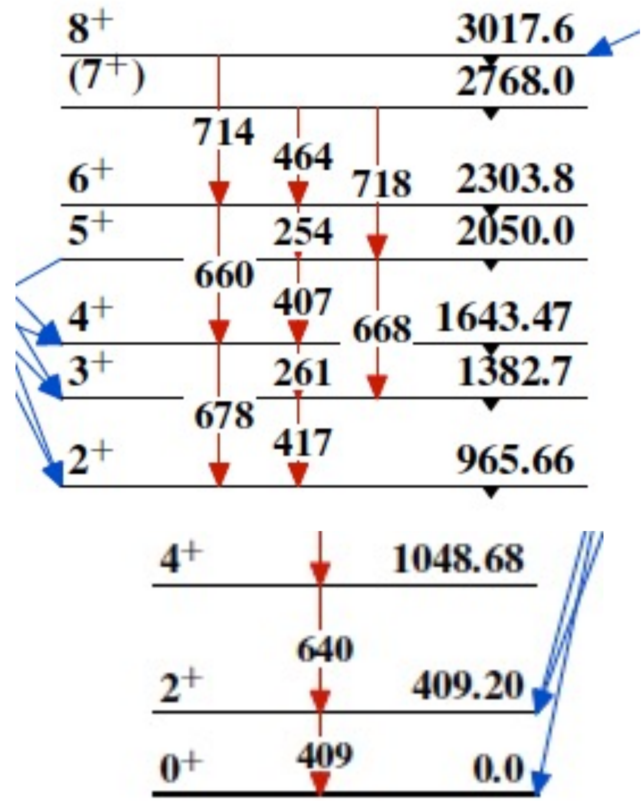


Fit to the 4 parameter Bohr Hamiltonian

Inclusion of core softness always destroys the TW pattern and leads to LW behavior.

# Triaxial Projected Shell Model

For even-even systems, the TPSM basis space is composed of projected 0-qp state (or qp-vacuum $|\Phi>$), 2-proton, 2-neutron, and 4-qp configurations, ...

$$\hat{P}^{I}_{MK}\,|\Phi>;$$
$$\hat{P}^{I}_{MK}\,a^{\dagger}_{p_1}a^{\dagger}_{p_2}\,|\Phi>;$$
$$\hat{P}^{I}_{MK}\,a^{\dagger}_{n_1}a^{\dagger}_{n_2}\,|\Phi>;$$
$$\hat{P}^{I}_{MK}\,a^{\dagger}_{p_1}a^{\dagger}_{p_2}a^{\dagger}_{n_1}a^{\dagger}_{n_2}\,|\Phi>, \quad \ldots$$

where the three-dimensional angular-momentum operator is given by

$$\hat{P}^{I}_{MK} = \frac{2I+1}{8\pi^2}\int d\Omega\, D^{I}_{MK}(\Omega)\,\hat{R}(\Omega),$$

Odd-A

$$\hat{P}^{I}_{MK}a^{\dagger}_{\pi_1}|\Phi\rangle,$$
$$\hat{P}^{I}_{MK}a^{\dagger}_{\pi_1}a^{\dagger}_{\nu_1}a^{\dagger}_{\nu_2}|\Phi\rangle,$$
$$\hat{P}^{I}_{MK}a^{\dagger}_{\pi_1}a^{\dagger}_{\pi_2}a^{\dagger}_{\pi_3}|\Phi\rangle,$$
$$\hat{P}^{I}_{MK}a^{\dagger}_{\pi_1}a^{\dagger}_{\pi_2}a^{\dagger}_{\pi_3}a^{\dagger}_{\nu_1}a^{\dagger}_{\nu_2}|\Phi\rangle \quad \ldots$$

The vacuum $|\Phi>$ is the BCS ground state with the deformations $\varepsilon$ and $\gamma$ as model parameters.
The Hamiltonian is of the paring + quadrupole-quadrupole type.

$$\hat{H} = \hat{H}_0 - \frac{1}{2}\chi\sum_{\mu}\hat{Q}^{\dagger}_{\mu}\hat{Q}_{\mu} - G_M\hat{P}^{\dagger}\hat{P} - G_Q\sum_{\mu}\hat{P}^{\dagger}_{\mu}\hat{P}_{\mu},$$

The coupling constants are determined by the self-consistency conditions

$$\Delta = G_M < P >, \quad G_Q = 0.16 G_M, \qquad 0.66\hbar\omega_0\varepsilon = \chi < Q\_0 >.$$

$\Delta$ is adjusted to the even-odd mass differences.
$\varepsilon$ is taken from $B(E2, 2^+_1 \to 0^+_1)$systematics or mean field equilibrium deformations.
$\gamma$ is adjusted to reproduce the $\gamma$ band head energy $E(2^+_2)$.

Step 1:
The triaxial angular momentum projected basis incorporates the correlations that generate 3D rotational behavior.
Step 2:
Diogalization takes care of the details, as small- vs. large- scale shape fluctuations.
Few parameters:
$B(E2, 2^+_1$->$0^+_1)$ fixes $\varepsilon$
$E(2^+_2)$ fixes $\gamma$.
Hamiltonian couplings constants from self-consistency.

MoI are microscopically fixed by the triaxial mean field.
Pauli Principle between valence particles and core obeyed.
Sufficient large configuration space incorporates dynamical effects.

N. Sensharma et al. PLB 792, 170 (2019)

First and second transverse wobbling states in $^{135}$Pr are well reproduced by TPSM

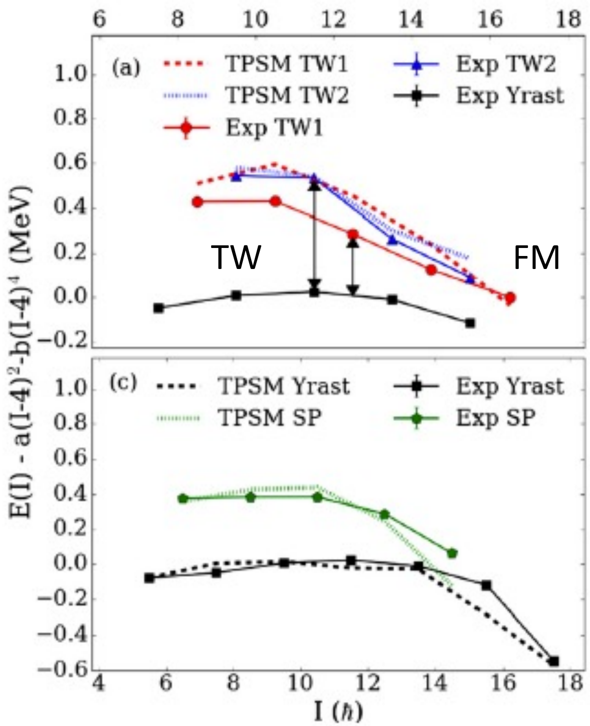


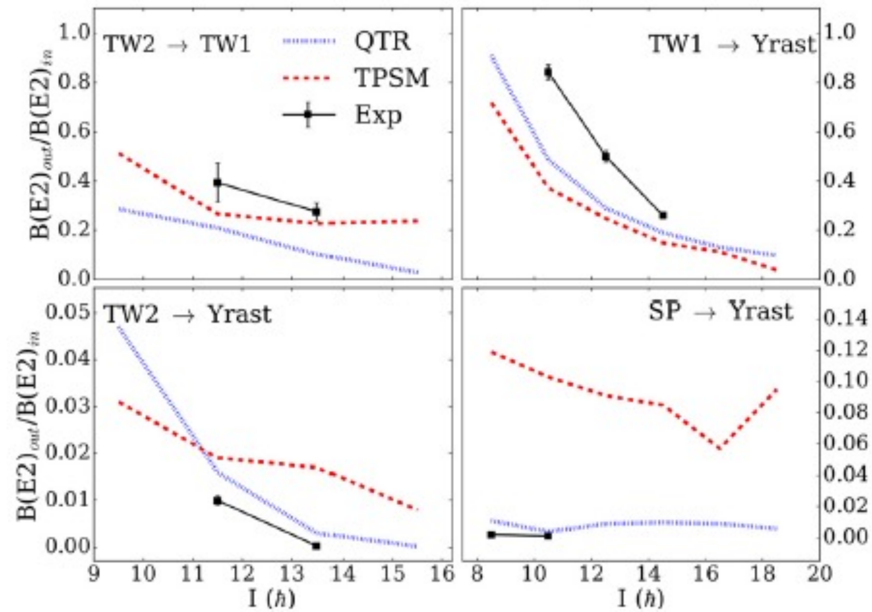


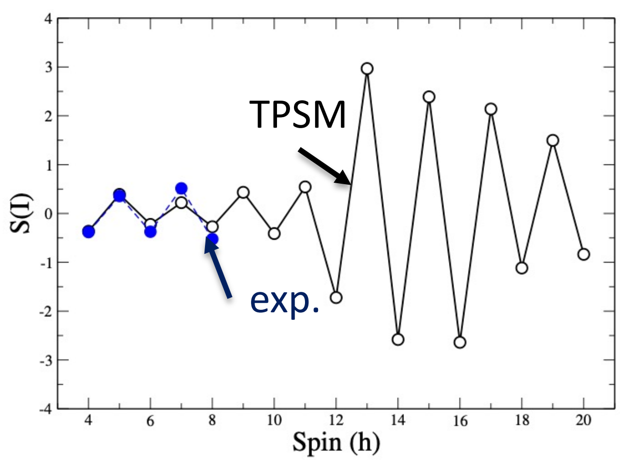


Even-I-down pattern of $\gamma$ softness in $^{134}$Ce reproduced by TPSM.
Apparent contradiction with TW in 135Pr resolved.
Exact antisymmetrization of TSPM states is crucial.

A. MUKHERJEE et al.,
PRC 107, 054310 (2023)

Tabassum Naz et al., NPA 979, 1 (2018)

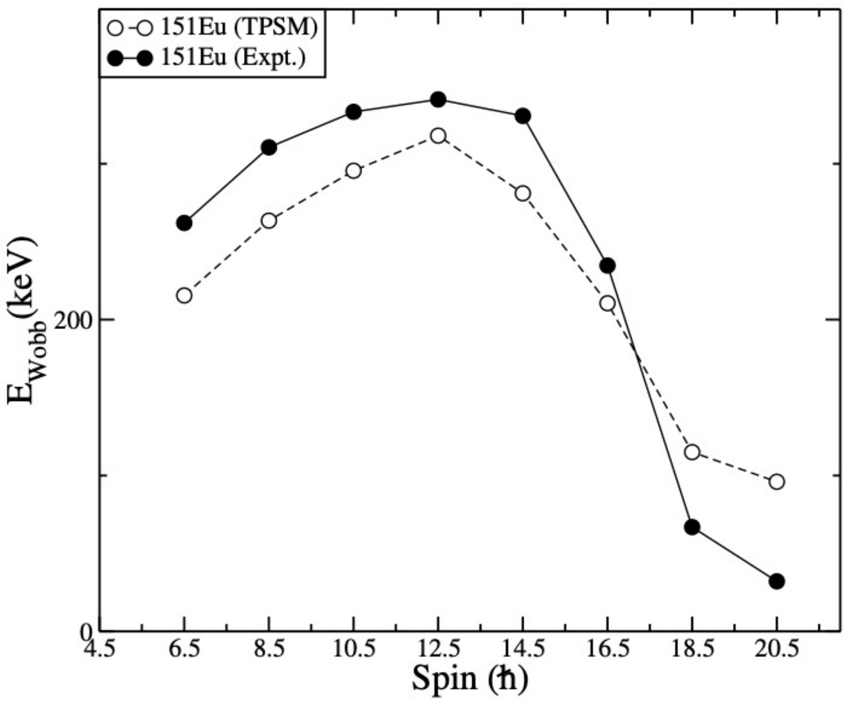


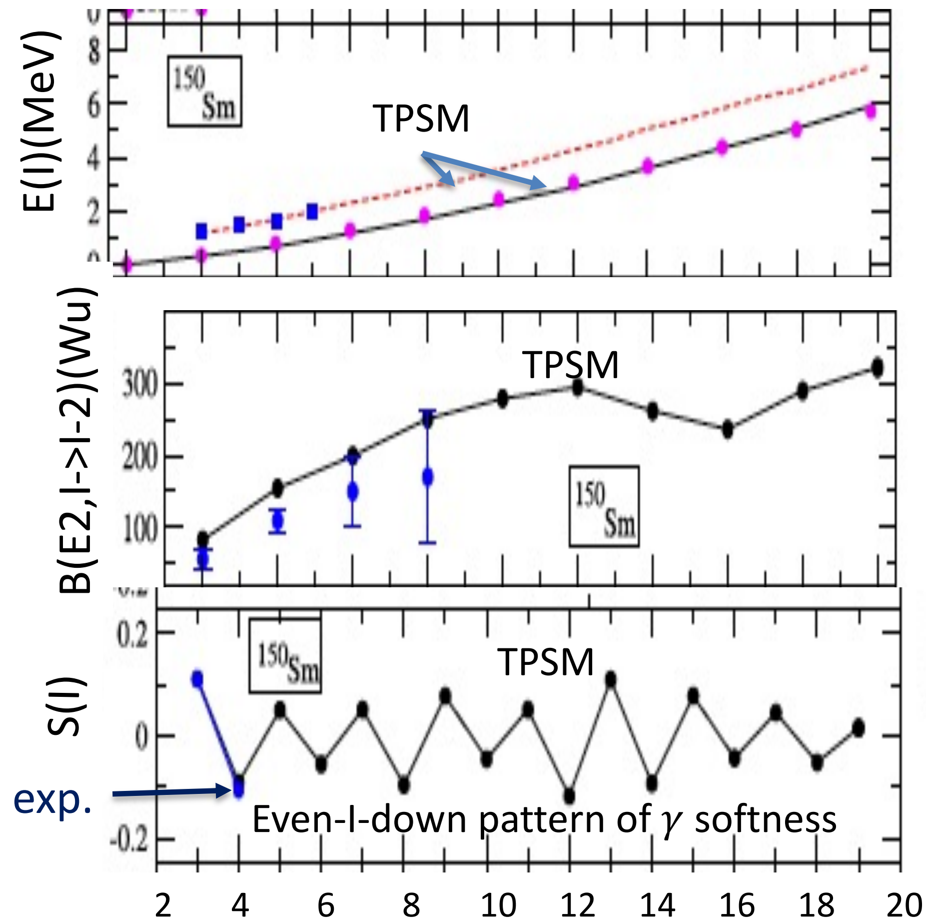


$^{151}_{63}Eu_{88}$ : a transverse wobbler is well described by TPSM with $\varepsilon = 0.20, \gamma = 27^o$.

$^{150}_{62}Sm_{88}$ : a $\gamma$ soft transitional nucleus is well described by TPSM with $\beta = 0.20, \gamma = 22^o$.

A. MUKHERJEE et al., PRC 107, 054310 (2023)

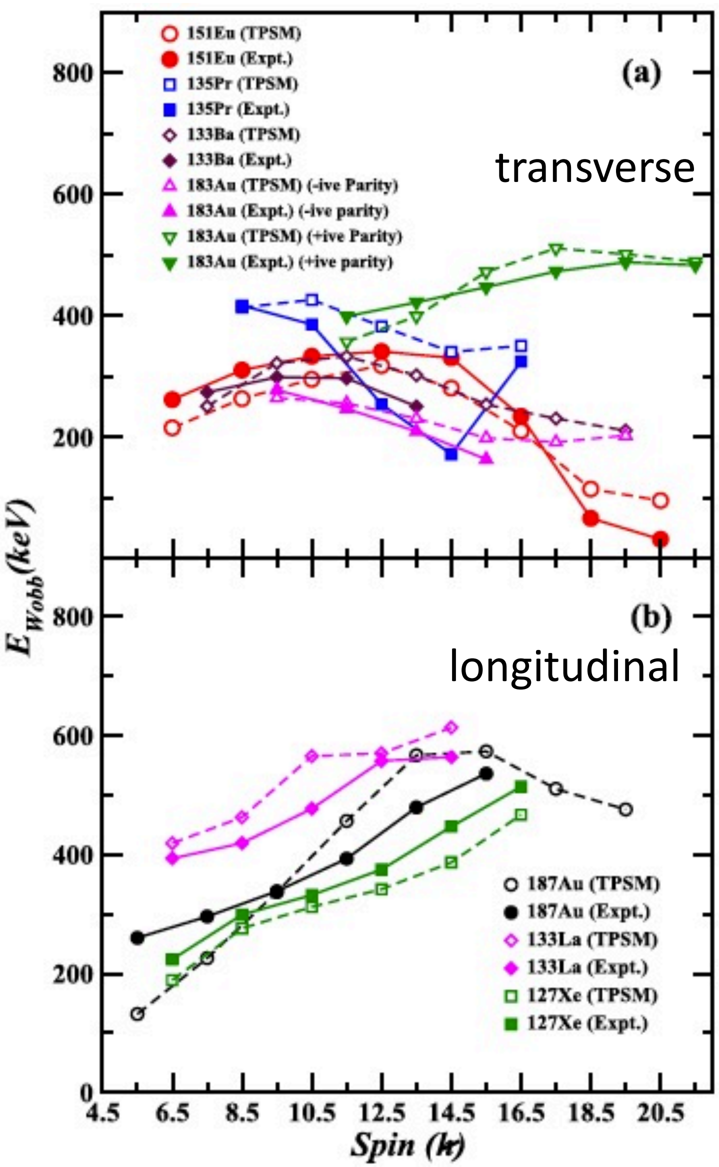


Impressive reproduction of the wobbling bands without explicit adjustment of the MoI.

$\gamma$ is the only adjusted parameter.

TABLE IV. The axial deformation parameter ($\epsilon$), triaxial deformation parameter $\epsilon'$, and ($\gamma$) employed in the calculation for odd-A nuclei. The axial deformation $\epsilon$ is taken from Ref. [53]. The asterisk $*$ shows $\epsilon$ for positive parity in $^{183}$Au nucleus.

| | $^{151}$Eu | $^{187}$Au | $^{135}$Pr | $^{133}$La | $^{127}$Xe | $^{133}$Ba | $^{183}$Au | $^{183}$Au |
|---|---|---|---|---|---|---|---|---|
| $\epsilon$ | 0.200 | 0.220 | 0.160 | 0.150 | 0.150 | 0.150 | 0.280 | 0.270* |
| $\epsilon'$ | 0.110 | 0.100 | 0.110 | 0.110 | 0.100 | 0.100 | 0.110 | 0.100 |
| $\gamma^0$ | 27 | 24 | 34 | 36 | 33 | 33 | 21 | 20 |

F. Q. Chen, C. Petrache, PRC 103, 064319 (2021)

# Transverse wobbler in $^{136}$Nd

$$|\Phi_\kappa\rangle \in \{|\Phi_0\rangle, \beta_i^\dagger \beta_j^\dagger |\Phi_0\rangle\},$$ $\pi h_{11/2}^2$ configuration

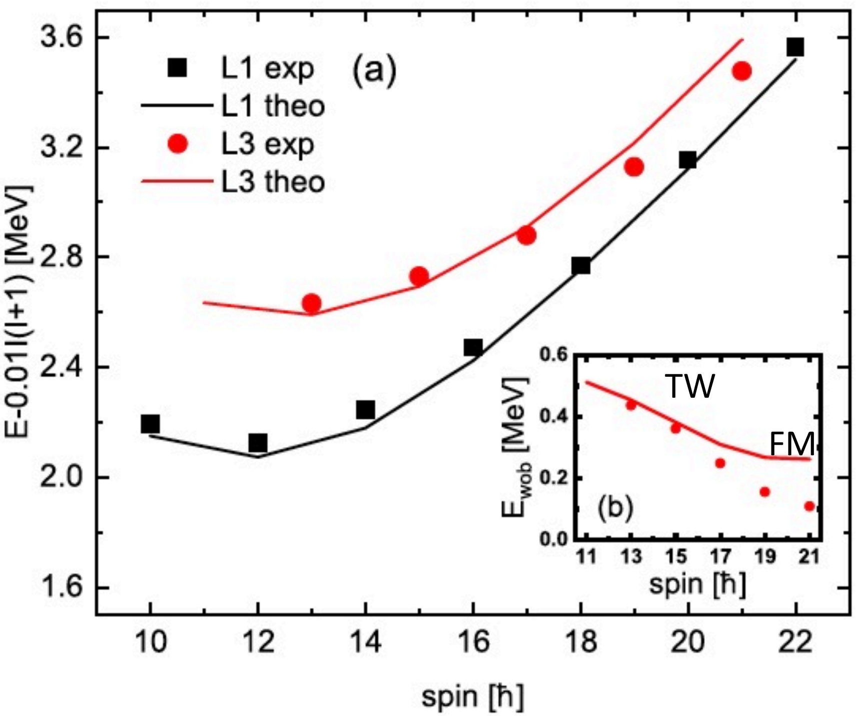


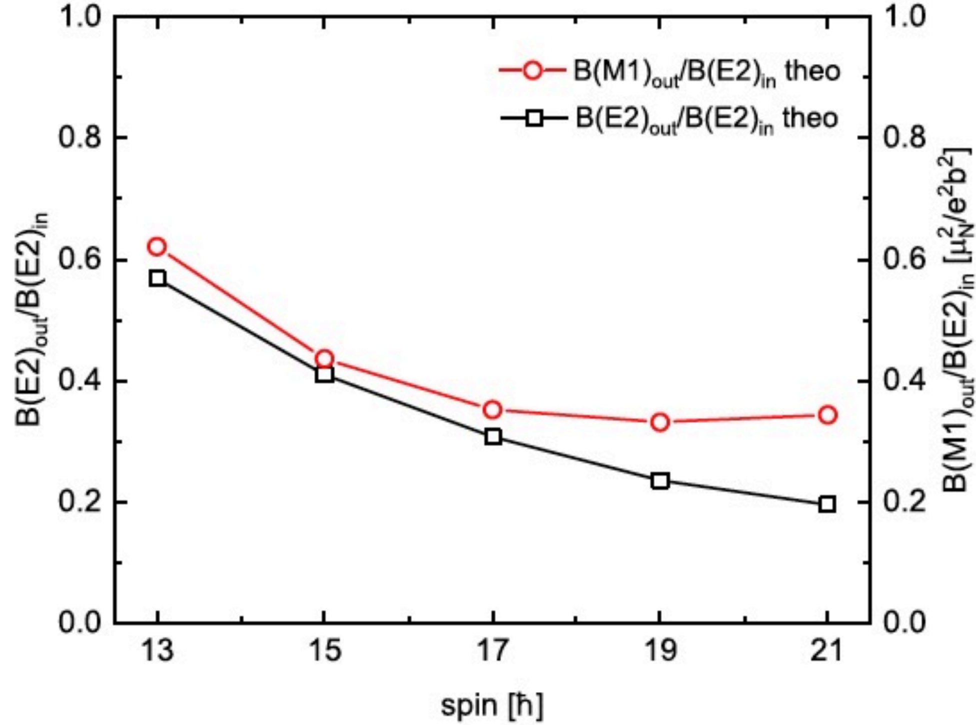

SCS maps

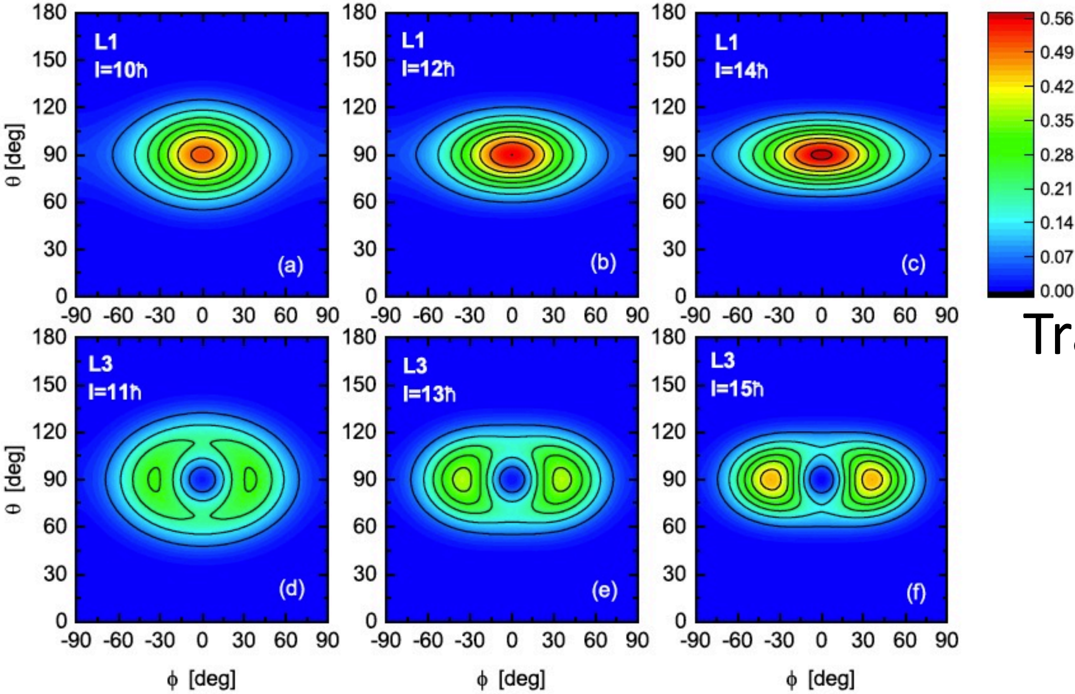


Transverse wobbling

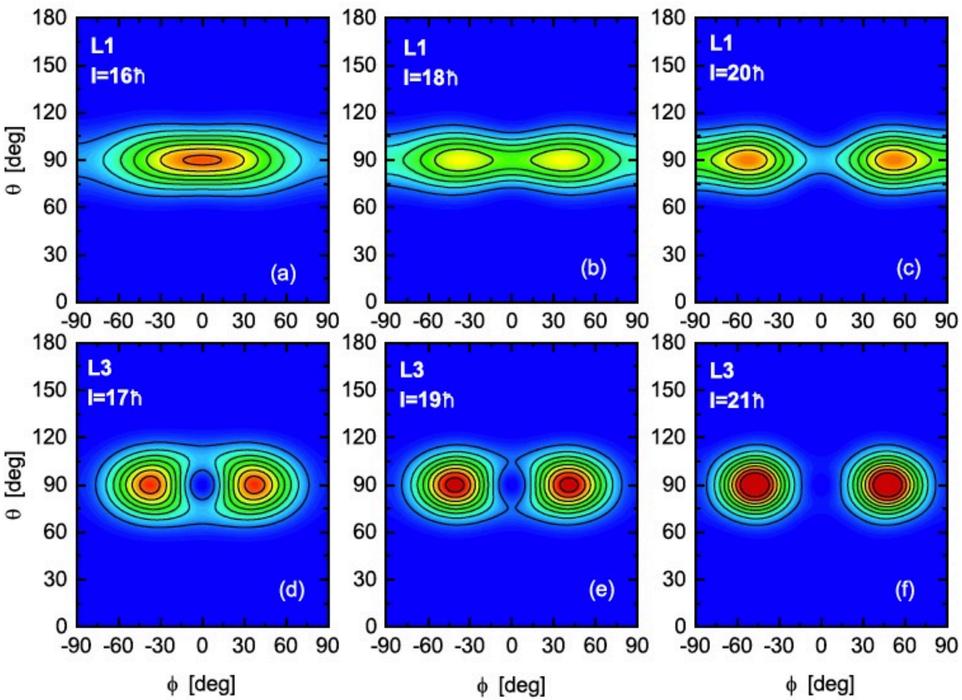


Transition to flip mode

LW regime not reached yet

# Summary

- Wobbling is a new collective mode: precessional motion of the charged triaxial body → enhanced E2 transitions
- Wobbling is specified by the corresponding classical orbits
- Transverse wobbling (TW): **J** revolves around the s– or l-axis transvers to m-axis of maximal moment of inertia, particle **j** approximately transverse → its excitation energy decreases with I.
- Longitudinal wobbling (LW): **J** revolves around the m-axis, particle **j** has transverse and longitudinal components → excitation energy increases with I.
- With increasing I, TW changes to LW via the Flip mode (FM), which represents flipping between tilted **J** directions, → excitation energy small, I independent
- Spin Coherent State maps display the topology of the quantum states.
- PTR well describes energies and E2, M1 transition probabilities, however sensitive to MoI input, ambiguities
- TPSM well describes energies and E2, M1 transition probabilities in both the valence particle + rotor type nuclei and $\gamma$ soft e-e neighbors.
- Promising tool, further development: more instructive visualization of physics content, better foundation on (cranked) mean-field theory, octupole correlations, shape coexistence, …